Punctuational ecological changes rather than global factors drive species diversification and the evolution of wing phenotypes in Morpho butterflies

Nicolas Chazot, Patrick Blandin, Vincent Debat, Marianne Elias, Fabien L. Condamine

Article type

Original article

Title

Punctuational ecological changes rather than global factors drive species diversification and the evolution of wing phenotypes in *Morpho* butterflies

Short running title

Dynamics of species and wing diversification

Authors

Nicolas Chazot[1,*], Patrick Blandin[2], Vincent Debat[2], Marianne Elias[2], Fabien L. Condamine[3]

Affiliations

[1] Department of Ecology, Swedish University of Agricultural Sciences, Ulls väg 16 75651 Uppsala, Sweden.

[2]Institut de Systématique, Évolution, Biodiversité, ISYEB - UMR 7205 – CNRS MNHN UPMC EPHE, Muséum national d'Histoire naturelle, Sorbonne Universités, 57 rue Cuvier CP50 F-75005, Paris, France.

[3]CNRS, UMR 5554 Institut des Sciences de l'Evolution (Université de Montpellier), Place Eugène Bataillon, 34095 Montpellier, France.

Corresponding author (*):

Nicolas Chazot, email: chazotn@gmail.com.

Acknowledgments

The authors have no conflict of interest to declare. F.L.C. has benefited from an "Investissements d'Avenir" grant managed by Agence Nationale de la Recherche (CEBA, ref. ANR-10-LABX-25-01). P.B benefited from the Programme Pluriformation "Etat et structure phylogénétique de la biodiversité actuelle et fossile".

Abstract

Assessing the relative importance of geographical and ecological drivers of evolution is paramount to understand the diversification of species and traits at the macroevolutionary scale. Here, we use an integrative approach, combining phylogenetics, biogeography, ecology, and quantified phenotypes to investigate the drivers of both species and phenotypic diversification of the iconic Neotropical butterfly genus *Morpho*. We generated a time-calibrated phylogeny for all known species and inferred historical biogeography. We fitted models of time-dependent (accounting for rate heterogeneity across the phylogeny) and paleoenvironment-dependent diversification (accounting for global effect on the phylogeny). We used geometric morphometrics to assess variation of wing size and shape across the tree, and investigated their dynamics of evolution. We found that the diversification of *Morpho* is best explained when considering variable diversification rates across the tree, possibly associated with lineages occupying different microhabitat conditions. First, a shift from understory to canopy was characterized by an increased speciation rate partially coupled with an increasing rate of wing shape evolution. Second, the occupation of dense bamboo thickets accompanying a major host-plant shift from dicotyledons towards monocotyledons was associated with a simultaneous diversification rate shift and an evolutionary "jump" of wing size. Our study points to a diversification pattern driven by punctuational ecological changes instead of a global driver or biogeographic history.

Keywords

Species diversification, phenotypic diversification, wing size, wing shape, geometric morphometrics, butterflies, *Morpho.*

Introduction

Investigating the rates of phenotypic evolution and the relationships between phenotypes and species ecology can shed light on the drivers of time and geographic patterns of diversity. Previous studies have demonstrated that rates of both species and phenotypic diversification vary widely through time and among clades at all taxonomic scales (e.g. Venditti *et al.*, 2011; Eastman *et al.*, 2011; Rabosky & Adams, 2012; Rabosky *et al.*, 2013; Rabosky *et al.*, 2014; Cooney & Thomas, 2020). These variations have resulted in the striking heterogeneity in species and phenotypic diversity observed across the tree of life. Such variations may eventually be coupled, indicating an interaction between the processes of species and phenotypic diversifications. Studies investigating such coupling have yielded contrasted results. Some of them support an association between specific and phenotypic diversification (e.g. in salamanders: Rabosky & Adams, 2012; fish: Rabosky *et al.*, 2013; vertebrates: Cooney & Thomas, 2020), while others found no support for this relationship (e.g. in lizards: Rabosky *et al.*, 2014; squirrels: Zelditch *et al.*, 2015; reef fishes: Price *et al.*, 2015; snakes: Lee *et al.*, 2016). For example in squirrels, Zelditch *et al.* (2015) suggested that species diversification was geographically driven while phenotypic diversification was ecologically driven, resulting in a decoupling of the two dynamics.

A correlation between species and phenotypic diversification rates is notably expected in some specific cases. For example, adaptive radiations – rapid adaptive diversification in a variety of ecological niches – are expected to produce bursts of diversification and phenotypic evolution especially during the initial stages of diversification (Schluter, 2000; Gavrilets & Losos, 2009). Speciation rate increases when a large number of ecological niches are vacant while phenotypes rapidly evolve in response to the diversity of ecological opportunities. Strong correlation between speciation rates and phenotypic diversification may also be found when the focal trait directly drives reproductive isolation. For example, the

evolution of male genitalia, involved in mating, may facilitate reproductive isolation between populations (see Langerhans *et al.*, 2016 for a review). Correlated dynamics leading to a lower rate of diversification can also be predicted. For example, if extinction probability is biased with respect to phenotype leading to a non-random loss of variation in a particular clade, both species and morphological diversity should show a correlated drop down (Foote, 1997). In this study, we assess the role of multiple ecological causes of variations in rates of species and wing diversification and the extent to which these variations are coupled, by focusing on the case of the butterfly genus *Morpho* (Nymphalidae).

The genus *Morpho* comprises 30 species (Blandin & Purser, 2013), which are amongst the largest butterflies in the Neotropics and are well known for their blue iridescent wing coloration. Several ecological factors have already been suggested as potential drivers of diversification and phenotypic evolution. Previous biogeographic estimations suggested that *Morpho* butterflies originated and started diversifying in the Andes (Penz *et al.*, 2012, Blandin & Purser 2013), before spreading across the Neotropics. There is also evidence that *Morpho* lineages separated early in their history into two microhabitats (DeVries *et al.*, 2010; Chazot *et al.*, 2016). One clade is composed of species that tend to fly high, often above the forest canopy, with some species typically harbouring gliding flight behaviour such as *M. cisseis* and *M. hecuba*. The remaining species mostly fly within the first meters above ground in the understory (DeVries *et al.*, 2010; Chazot *et al.*, 2016). Finally, according to Cassildé *et al.* (2010) and Penz *et al.* (2012), the genus *Morpho* was ancestrally feeding on monocotyledons, and two major host-plant shifts occurred during its diversification: after the first divergence event, one of the two clades shifted to dicotyledon host-plants and, within this clade, a subclade subsequently reversed to the monocotyledons.

Here we focus on the wings of *Morpho*, which are at the crossroad of multiple selective pressures and tightly linked to species diversification. Typically, wing colour

patterns can be involved in camouflage, aposematism or courting behaviours (Naisbit *et al.*, 2001; Merrill *et al.*, 2011). Wings also allow flight, enabling dispersal, foraging, predator escape, mating or host-plant searching (Dudley, 2002). Hence butterfly wings are under strong natural and/or sexual selection and may be associated with variations of speciation rate (Ortiz-Acevedo *et al.*, 2020). Both size and shape are important aspects of wing morphology. They both strongly affect the performance of flight behaviours (Dudley, 2002; Le Roy *et al.*, 2019) and therefore might be closely associated to habitat use, dispersal strategies or host-plant searching. Besides, fore and hind wings can be functionally differentiated, for example during flight (Grodnitsky *et al.*, 1994; Le Roy *et al.*, 2020), which may lead to different patterns of diversification.

To investigate whether species and phenotypic diversification dynamics are coupled and to identify potential drivers of variations, we inferred a time-calibrated molecular phylogeny of the genus that we combined to a dataset of geographical distributions and morphometric measurements of wing size and shape. We applied an integrative approach and addressed the following questions: (1) Have rates of phenotypic diversification varied across the tree? We investigated potential variations in rate of phenotypic diversification among clades using phenograms and models of trait evolution to compare evolutionary rates for wing size and shape. (2) Is species diversification better explained by global processes or clade-specific (ecological) factors? First, we fitted different models of species diversification testing for global drivers of diversification, specifically past temperatures and Andean orogeny. Second, we compared these global drivers to models in which species diversification varied according to clade-specific ecological factors (microhabitat and major shifts of host-plants) and/or variations of phenotypic diversification identified in the first step. (3) Can we explain the variations in diversification rates by historical biogeography? We performed ancestral areas estimation in order to assess whether variations in phenotypic

130 evolutionary rates or species diversification rates may be associated with specific
131 biogeographic events.
132
133 **Material and methods**
134 ***Time-calibrated phylogeny***
135 Phylogenetic relationships and divergence time were inferred with Bayesian inference. We
136 concatenated DNA data for one mitochondrial (COI) and four nuclear genes (CAD, EF-1α,
137 GAPDH and MDH) using published sequences (Cassildé *et al.*, 2012; Penz *et al.*, 2012;
138 Chazot *et al.*, 2016) retrieved from GenBank, generating a molecular dataset of a total length
139 of 5001 nucleotides. Our dataset includes all *Morpho* species (i.e. 30 species *sensu* Blandin,
140 2007). *Morpho helenor*, which harbours many subspecies, is distributed throughout the entire
141 Neotropical region, resulting in unresolved biogeographic reconstructions in preliminary
142 analyses. To help resolving the biogeographic inferences, *M. helenor* was represented in the
143 biogeographic analyses by six subspecies that each occupies a distinct Neotropical area. For
144 all other analyses, we pruned all subspecies of *M. helenor* but one in order to keep a single
145 branch for the species. We also included 11 outgroups to root and calibrate the tree (see
146 Supporting Information S1) on the basis of the most comprehensive nymphalid phylogeny to
147 date (Wahlberg *et al.*, 2009).
148 To simultaneously estimate the topology and branching times of the phylogeny we
149 used a Bayesian relaxed-clock approach as implemented in *BEAST* 1.8.2 (Drummond *et al.*,
150 2012). To choose the best partitioning strategy and the corresponding substitution models, we
151 ran *PartitionFinder* 1.1.1 (Lanfear *et al.*, 2012) allowing all possible partitions and models
152 implemented in *BEAST*. Three subsets were defined: the first included position 1 and 2 of all
153 genes and followed a GTR+I+Γ model, the second included position 3 of all nuclear
154 fragments and followed a GTR+Γ model, and the third including the position 3 of the

mitochondrial fragment and followed a TrN+Γ model. We implemented an uncorrelated lognormal relaxed clock model. Given the lack of fossils in the focal clade, we relied on secondary calibrations to calibrate the molecular clock. Penz *et al*. (2012) calibrated the divergence between *Morpho* and its sister groups using a unique calibration point from Wahlberg *et al.* (2009), and a normal distribution for the corresponding prior. However, Sauquet *et al.* (2012) showed that using a single secondary calibration prior could yield biased estimates. Hence, we used a set of seven calibrations defined by uniform priors bounded by the 95% credibility intervals (95% CI) estimated by Wahlberg *et al.* (2009) (see Supporting Information S1). We implemented a Yule process for the tree prior, and we ran the phylogenetic analyses for 30 million Markov chain Monte Carlo (MCMC) generations. We checked for chain convergence using *Tracer* 1.6, as indicated by effective sample size (ESS) values. Finally, we used *TreeAnnotator* 1.8.2 (Drummond *et al.*, 2012) to select the maximum clade credibility (MCC) tree with median age values calculated from the posterior distribution of branch lengths, applying a 20% burn-in.

Morphological data

Our morphological dataset (published by Chazot *et al.* 2016) consists in the size and shape of the fore and hind wings, as assessed by morphometric measurements. A total of 911 collection specimens of both sexes and representing all *Morpho* species were photographed. Wing shape was described using landmarks and semi-landmarks placed at vein intersections and wing margins, respectively (see Chazot *et al.*, 2016 for details), which were superimposed with *tpsRelw* (Rohlf, 1993). Wing size was measured using the log-transformed mean centroid size per species. Importantly, for analyses involving wing shape we used the residuals of a multivariate regression of species mean Procrustes coordinates on species mean centroid size (log-transformed), which allows focusing on the non-allometric

shape variation. Similar analyses were performed separately on the fore and hind wings. All analyses were performed on males and females separately. As we found divergent patterns among sexes, we show the results for males and females separately. No female *M. niepelti* was available. This species was therefore pruned from the tree for all analyses involving female data.

Dynamics of phenotypic diversification

We investigated whether the evolutionary rates of wing size and shape have varied among subclades across the phylogeny.

Wing size – We first visualized the evolution of traits through time using the *phenogram* function in *PHYTOOLS* 0.5-20 (Revell, 2012), which represents the trait values inferred at each node along a time axis. Second, we investigated the dynamics of wing size evolution across lineages using the method implemented in the function *rjmcmc.bm* available in *GEIGER* 2.0.6 (Harmon *et al.*, 2008; Eastman *et al.*, 2011) for univariate traits. This method uses Bayesian analyses and reversible-jump MCMC to infer the number and the location of shifts of morphological diversification dynamics. We fitted and compared three different models of trait evolution: (1) a single-rate Brownian model (BM); (2) a relaxed model of Brownian evolution in which a trait evolved according to distinct Brownian-motion models across the tree (rBM); and (3); a model in which trait evolution can also occur at punctuational "jumps", i.e. brief periods of rapid evolution at any branch in the phylogeny (jBM). We ran models on both the MCC and a posterior distribution of trees. For the MCC tree analysis, we ran for each model one MCMC of 30 million generations, sampling every 3,000 generations. We checked for convergence of each run using *CODA (*Plummer *et al.* 2020*)*, and computed the ESS. We applied a 25% burn-in and compared the three models using the Akaike's Information Criterion for MCMC samples *aicm* and *aicw* implemented in

205 *GEIGER* (Supporting Information S2). To assess the robustness of the inferences to branch
206 length uncertainties, we repeated the analysis on a posterior distribution of trees and
207 summarized the results. We sampled 100 trees with a topology identical to that of the MCC
208 tree from the posterior distribution. For each tree, we ran the three models but reduced the
209 MCMC to 10 million generations, calculated the *aicm* score, the mean *aicm* pairwise
210 differences between models and the position of rate shifts and jumps. We summarized the
211 results by calculating the frequency of shifts and jumps at nodes across the posterior
212 distribution. These results are hereafter referred to as shift/jump posterior tree frequencies.
213 *Wing shape* –Some authors have used the scores on the first PC-axis as a univariate
214 shape measure (e.g. Rabosky *et al.*, 2014; Thacker, 2014) to investigate shifts in evolutionary
215 rates for multidimensional traits, but this may lead to spurious results (Uyeda *et al.*, 2014).
216 We rather investigated variations in rates of shape evolution across the phylogeny in a
217 multivariate way using the function *compare.evol.rate* from *GEOMORPH* (Adams, 2014;
218 Denton & Adams, 2015). It allows testing whether species assigned to different ecological
219 factors have significantly different rates of shape evolution, by comparing the ratio between
220 the rates of each group to a null distribution of ratios obtained through simulation of a unique
221 neutral evolutionary rate (two or more factors can be tested). When more than two factors are
222 included, the function performs a global test for the significance of the multiple rates model
223 compared to a one-rate model, but also assesses the significance of differences among each
224 pair of factors. We used this factor assignment to define monophyletic subgroups with
225 potentially divergent evolutionary rate from the background rate. We first tested all models
226 with one shift, i.e. all species belonging to one subclade (each subclade had a minimum of
227 three species) are assigned to one group, and the rest of the species assigned to another group.
228 If two or more subclades were identified as having a rate of evolution significantly different
229 from that of the background, we identified the subclade with the highest ratio (hence the

230 greatest shift). Then we ran again *compare.evol.rate* on all possible combinations of two
231 shifting subclades that include the first identified shift. A two-shift model was considered
232 significant if at least the two shifting subclades showed a significant difference with the
233 background rate when considering the pairwise comparisons. Given the relatively small size
234 of our phylogeny, we limited our analysis to two shifts (Supporting Information S3-S4). As
235 for wing size, we repeated the analysis on both the MCC tree and a posterior distribution of
236 trees with identical topologies. We summarized the results from the posterior distribution by
237 calculating the frequency of significant shifts at nodes across the trees, and refer to these as
238 posterior tree frequencies.
239
240 ***Dynamics of species diversification***
241 We compared two types of species diversification models: (1) diversification rates varying
242 according to global factors, i.e. factors virtually affecting all lineages, and (2) diversification
243 rates varying at specific clades characterized by clade-specific ecological factors. For each
244 type we investigated different factors (see below). All models were compared using their AIC
245 scores to identify the model that best explains the diversification of the genus *Morpho*.
246 *Global drivers of diversification* – We tested the role of temperature fluctuations and
247 of the paleo-elevation of the Andes on species diversification by using birth-death models
248 that allow speciation and extinction rates to vary according to a past environmental variable
249 itself varying through time (Condamine *et al.*, 2013). For each paleoenvironmental variable,
250 we designed three models to be tested: *(i)* the speciation rate varies exponentially with the
251 environment and the extinction rate is constant, *(ii)* the speciation rate is constant and the
252 extinction rate varies exponentially with the environment, and *(iii)* both speciation and
253 extinction rates vary exponentially with the environment. We repeated these three models
254 with a linear dependence to the environmental variable, instead of exponential dependence.

For temperature we relied on the well-known Cenozoic temperature dataset published by Zachos *et al.* (2008). The orogeny of the Andes is a highly complex process, with important differences in uplift tempo and mode from the south of Central Andes to Northern Andes (Blandin & Purser, 2013, and references therein). Several general phases have been identified from the late Eocene to present, but they are difficult to synthetize in a unique model. As Blandin & Purser (2013) suggested that the early diversification of the *Morpho* occurred along the proto-Central Andes, we used the model of surface uplift inferred by Leier *et al*. (2013) for the eastern cordillera of the southern Central Andes to test the possible influence of Andean orogeny on the diversification of the *Morpho*. We used the R-package *PSPLINE* 1.0-17 to reconstruct smooth lines of the paleo-data for each environmental variable. The smooth line is introduced in the birth-death model to represent the variation of the environment through time. Given the dated phylogeny, the model then estimates speciation and extinction rates, as well as their respective variations according to the environment (Condamine *et al.*, 2013). These analyses were performed on 200 trees randomly sampled from the posterior distribution generated by BEAST.

Clade-specific drivers of diversification – We assessed whether the diversification rates across the genus *Morpho* have varied among specific clades using models of time-dependent diversification. To do so we used the method developed by Morlon *et al.* (2011), which allows partitioning diversification rates into independent dynamics (a backbone and different subclades). We compared different partitioning schemes according to three events: (1) the microhabitat change (from understory to canopy), (2) the shift of wing shape evolutionary rate, and (3) the reverse shift to monocotyledon host-plants (also identified as a punctuational evolutionary jump of wing size at the stem). Because the evolutionary rate shift of wing shape is nested within the microhabitat shift (see Results), we could not test both combined. Instead, each of those shifts was combined to the monocotyledon host-plant shift

with a two-shift model of diversification rate. For each subclade and the remaining backbone, we fitted the following models: *(i)* constant speciation rate and no extinction, *(ii)* time-dependent speciation rate and no extinction, *(iii)* constant speciation and extinction rates, *(iv)* time-dependent speciation rate and constant extinction rate, *(v)* constant speciation rate and time-dependent extinction rate, and *(vi)* time-dependent speciation and extinction rates. Time dependency was modelled using an exponential function of time. The stem branch of each subclade was included in the subclades and excluded from the backbones but we kept the node of the divergence (speciation event) of the subclade within the backbones. The root of the tree was excluded from the analyses. The analysis was performed on the MCC tree, since partitioning the tree requires defining clades *a priori*, which entails a fixed topology.

Historical biogeography

To assess where and when diversification occurred, we estimated ancestral areas using the dispersal-extinction-cladogenesis (DEC, Ree and Smith, 2008) model as implemented in the R-package *BioGeoBEARS* 0.2.1 (Matzke, 2014). The analyses were performed using the MCC tree (outgroups removed) and included six subspecies of *M. helenor* (each subspecies was assigned to its current distribution).

The distribution of *Morpho* is restricted to South America and Central America (all Neotropics except the Caribbean Islands). A geographic model was incorporated to include operational areas, defined as geographic ranges shared by at least two or more species and delimited by geological, oceanic or landscape features, which may have acted as barriers to dispersal. The model comprised 7 component areas: (A) Central America, (B) trans-Andean South-America, (C) slopes of northern Andes, (D) eastern slopes of central Andes, Orinoco-Amazonian basin north of the Amazon, including the Guyanas, (E) Amazonian basin, south of the Amazon River, and (F) Atlantic forest.

An adjacency matrix was designed whilst taking into account the geological history and the biological plausibility of combined ranges (Supporting Information S6). Distributional data were compiled from monographies (Blandin, 2007). We excluded distribution margins overlapping with adjacent areas. For example, *M. marcus* and *M. eugenia* are mainly found in lowlands but their distributions reach the Andean slopes up to altitudes of 700-800m. Nevertheless, we did not consider these as species occupying the Andean biogeographic areas. By contrast, a species such as *M. sulkowskyi*, which occurs between 1500 and 3500m high in the Andes was considered as an Andean species. We also set a maximum of 3 areas per node to be constitutive of an ancestral range. We fitted two different DEC models, one that assumed equal dispersal probabilities among all areas and one that included time-stratified matrices of varying dispersal probabilities (Supporting Information S6). We compared the likelihoods of both reconstructions to select the model best explaining the current pattern of species distribution.

Results

Divergence times

We estimated that the genus *Morpho* diverged (stem age) from its sister genus *Caerois* 38.05 Ma (95% CI=35.48-39.20 Ma) and the first event (crown age) of diversification was recovered at 28.12 Ma (95% CI=25.22-31.24 Ma; Supporting Information S1). These divergence time estimates are slightly older than those estimated by Penz *et al.* (2012) and Chazot et al. (2019) who found an average divergence from *Caerois* around 32.00 Ma and 29.08 Ma respectively. This difference probably results from prior choices for calibrating the trees (see Material and Methods).

Dynamics of phenotypic diversification

330 *Wing size* – Both analyses on the MCC and posterior distribution of trees found
331 similar results. We found no support for any shift in rate of wing size diversification.
332 However, we found support for an evolutionary jump. For females the model jBM was highly
333 supported for both wings, with a highly probable evolutionary jump at the root of the clade
334 including the species *M. absoloni*, *M. aurora*, *M. zephyritis*, *M. rhodopteron*, *M. sulkowskyi*,
335 *M. lympharis*, *M. aega*, and *M. portis* (subclade *portis*; posterior tree frequency [PF] of 0.99,
336 Supporting Information S2). Phenograms show that in this subclade, female wings are on
337 average 34% smaller than in the other *Morpho* species for both fore and hind wings (Fig. 1).
338 This is all the more striking as the sister clade (including *M. amathonte*, *M. menelaus*, and *M.*
339 *godartii*) contains some of the largest species of the genus (e.g. *M. amathonte* has a wingspan
340 of 10–15 cm). For males, the *portis* clade exhibits the same trend, but the support for the
341 evolutionary jump is lower than for females ($PF_{forewing}$=0.76, $PF_{hindwing}$=0.71, respectively,
342 Supporting Information S2). Males wings in the portis clade were on average 30 and 32%
343 smaller for fore and hind-wing respectively.
344 *Wing shape* – We found support for two shifts of evolutionary rate for male hindwing,
345 in both cases towards lower rate of evolution. These subclades encompass *M. helenor*, *M.*
346 *achilles*, and *M. granadensis* (Fig. 2, Supporting Information S3) on one side, and *M.*
347 *godartii*, *M. menelaus*, and *M. amathonte* on the other. This result was supported by the
348 analyses with the MCC tree. The analyses performed on the posterior tree distribution found
349 a moderate support for these shifts, with PF of 0.62 and 0.77, respectively. For females and
350 for both wings the subclade encompassing *M. theseus*, *M. amphitryon*, *M. telemachus* and *M.*
351 *hercules* exhibited the greatest shift (highest ratio) (Fig. 2, Supporting Information S4). This
352 shift corresponds to a large increase in rate of evolution (forewing ratio=181.74, hindwing
353 ratio=184.49 in the MCC analysis), i.e. wing shape evolving faster within this group than the

354 other *Morpho*. This result was strongly supported by posterior distribution analyses, with PF
355 of 0.96 and 0.99 for fore and hind-wing, respectively.
356
357 ***Dynamics of species diversification***
358 *Global drivers of diversification* – In the best model accommodating for Central
359 Andean paleo-altitudes, speciation rates were negatively dependent on the paleo-altitude and
360 extinction rates were constant (Table 2a). This model leads to a continuous decrease in
361 speciation rate towards the present, suggesting that *Morpho* diversification was high during
362 the early stages of the orogeny but the rise in altitude did not lead to any increased
363 opportunities for speciation over time. We also found a significant correlation between
364 *Morpho* diversification and temperature compared to a null model (Table 2b). The best fitting
365 paleoclimatic model indicates that speciation rate was positively correlated with temperature
366 variation while extinction remained constant. This means that speciation rate was high during
367 the initial stages of diversification when the temperatures were warmer but globally
368 decreased during the last 14 million years as the Earth cooled down (Zachos *et al.*, 2008).
369 *Clade-specific dynamics of diversification* – The best-partitioned models included a
370 shift of diversification rate for the host-plant shift and for the canopy shift (Table 3,
371 Supporting Information S5). Under this configuration, the diversification of the clade that
372 shifted to monocotyledon host-plants was best modelled by a speciation rate decreasing
373 through time combined with no extinction, and the diversification of the canopy clade was
374 best modelled by a constant speciation rate with no extinction (Table 3, Fig. 3). For the
375 remaining backbone lineages the best fitting model was a time-dependent speciation and
376 extinction. The resulting net diversification rate (speciation minus extinction) of this
377 backbone was high during the very early stages of diversification but rapidly decreased
378 through time and became negative *ca.* 25 Ma, implying a declining diversity (Fig. 3). Around

22 Ma, the net diversification rate became positive again and reached zero at the present. This model of partitioned dynamics of diversification outperformed any model involving a global driver of diversification. Indeed, the multi-rate time-dependent model better fit the diversification of *Morpho* (AICc=191.69) than the temperature-dependent model (AICc=197.3, ΔAIC=5.61) and the altitude-dependent model (AICc=199.0, ΔAIC=7.31).

Historical biogeography

The model of biogeographic estimation with user-specified dispersal probabilities yielded a worse fit than the model with equal dispersal probabilities (likelihood with time-stratified dispersal multipliers: DEC_{strat}=-143.41; likelihood without time-stratified dispersal multipliers DEC_{null}=-140.75) and the ancestral state estimations involved some important differences. In both reconstructions the root state was highly unresolved. In the DEC_{null} model (highest likelihood), the area with the highest probability at the root was the southern part of the Amazonian Basin, *ca.* 28.1 Ma. The early divergence of the clade containing *M. marcus* and *M. eugenia* was accompanied by a colonization of the northern part of the Amazonian Basin (Fig. 4). The ancestor of the remaining group of *Morpho* occupied the Central Andes. This lineage then diverged into an Andean and an Amazonian lineage. This event (21.8 Ma) was also accompanied by a shift in microhabitat use: flight in low forest strata (understory) for the Andean lineage, and flight high above ground up to the canopy for the Amazonian lineage. The Andean lineage began a long-term occupation of the Central Andes with local diversification (12 nodes inferred occupying the Central Andes after the initial dispersal event). Around 11-12 Ma, cis-Andean (east of the Andes) recolonizations of Amazonia and the Atlantic Forest happened in three lineages. *M. polyphemus* is an intriguing case as it diverged 20.8 Ma from an Andean ancestor, but nowadays occupies Central America, whose connection to South America is often considered to be only completed

404 during the last 4-3 million years. This implies either an earlier dispersal route of emerging
405 Central America or a more recent dispersal with a joint extinction in the South American
406 landmass. Overall, Northern Amazonia and the Northern Andes appear to have been
407 colonized recently, during the last 5 million years (Fig. 4).
408
409 **Discussion**
410 In this study we aimed at investigating the large-scale patterns of diversification of the
411 *Morpho* butterflies by jointly evaluating the dynamics of species and phenotypic
412 diversification, to assess whether they are coupled or not and to test whether they correlate
413 with clade-specific factors and/or biogeographic events. Our results show that ecological
414 idiosyncrasies predominantly explain the pattern of diversification, instead of global (tree
415 wide) factors. These ecological changes affected to a large extent both species and
416 phenotypic diversification, leading to the partial coupling of both dynamics. Based on the
417 amount of information currently available on the ecology of *Morpho* we discuss the potential
418 role of several ecological and biogeographic events as well as the correlation with phenotypic
419 diversification in explaining these variations among groups.
420
421 *Study limitations*
422 A number of limitations have to be mentioned before discussing our results. Focusing on a
423 small clade allowed us to combine multiple ecological, morphological and historical
424 components thereby providing a deep understanding of the *Morpho* history. Although we
425 sampled all known species for both the molecular phylogeny and morphological traits, our
426 comparative analyses probably lack power as a result of both the small number of taxa (30
427 species) and the phylogenetic distribution of the traits of interest. Both microhabitat shift and
428 host-plant shift (towards monocotyledons) are single events happening at the root of a single

clade each and we lack phylogenetically independent similar shifts. Typically, we found an evolutionary jump in wing size to be associated with a shift from dicotyledons to monocotyledons host-plants. Further work addressing this pattern at a larger phylogenetic scale will be necessary to assess the generality of our finding. Furthermore, the reliability of birth-death models to assess the diversification dynamics from phylogenies of extant taxa is debated (e.g. Quental & Marshall, 2010; Louca & Pennell, 2020). We thus remain cautious with our estimation of the diversification dynamics and the interpretation of the different models tested. In particular, we avoided interpreting the speciation and extinction rates independently to focus only on the net diversification dynamics. Finally, the timing and magnitude of the Andean surface uplift is also controversial (see for example Evenstar *et al.*, 2015, and references therein; Fiorella *et al.*, 2015). We based our test on the reconstruction proposed by Leier *et al.* (2013) that focused only on the eastern cordillera of the Central Andes where the *Morpho* diversity is the highest, but had a large uncertainty in their paleo-altitude estimations. The Andean orogeny was spatially and temporally heterogeneous (Horton, 2018), which makes the use and interpretation of the paleoaltitude-dependent diversification model difficult (Condamine *et al.*, 2018). Those limitations should thus be kept in mind throughout the following discussion of the drivers of diversification, and the signal of declining diversity in particular.

Early Andean diversification not directly driven by Andean uplift

The diversification of the genus *Morpho* in the Andes could have happened either simultaneously with the uplift – a scenario where speciation is driven by the increasing heterogeneity of ecological conditions with new altitudes (Lagomarsino *et al.*, 2016) – or decoupled from orogenesis – a scenario where a clade radiates across a range of altitudes already established through adaptations to ecological conditions (e.g. climate, host-plants,

predators). Our results support the second hypothesis. We found that a model of diversification rate responding to paleo-altitude performed worse than the clade-specific diversification models (Tables 2 and 3), which means that neither global speciation nor extinction rate variations are well explained by the paleo-altitudes of the Central Andes. From a biogeographic point of view, 16 extant species (over 30) are almost restricted to the lowlands, while only six extant species have a distribution strictly restricted to the Andes. Yet, from the Oligocene-Miocene boundary to middle Miocene periods (23.5 to 11.6 Ma), 11 nodes out of 14 were inferred to be at least in the Central Andes from our biogeographic estimation (Fig. 4). Combined to the hypothesis that the *Morpho* probably originated in the foothills of the proto-Central-Andes, it is undeniable that the Central Andes played an important role in the early diversification of *Morpho*. During the second half of their evolutionary history, these lineages dispersed and diversified out of the Central Andes.

In contrast with the pattern of Central Andean diversification described above, the Northern Andes appear to have played only a minor role: while Northern Andean uplift likely established a barrier in three instances, resulting in cis- and trans-Andean *Morpho* lineages (Fig. 4), no major diversification was associated with the periods of Northern Andean uplift (Blandin & Purser, 2013). This absence of local diversification in the Northern Andes is a major difference compared to other butterflies such as the Ithomiini in which several groups repeatedly diversified at a high rate in the Northern Andes such as the genera *Napeogenes* (Elias *et al.*, 2009), *Oleria* (De-Silva *et al.*, 2016), *Hypomenitis* (Chazot *et al.*, 2016) or *Pteronymia* (De-Silva *et al.*, 2017).

Diversification driven by host-plant evolution may be an alternative explanation for the early diversification of *Morpho*. Penz and DeVries (2002) and Cassildé *et al*. (2010) suggested that monocotyledons were the ancestral host-plants of the genus *Morpho*, probably because at the time it was admitted that *M. marcus* larvae feed on monocotyledons

(Constantino, 1997). However, we now know that *M. marcus* very probably feeds on Fabaceae (e.g. *Inga auristellae*; Ramírez-Garcia *et al*., 2014; Vásquez Bardales *et al.*, 2017), and *M. eugenia* certainly feed on Caesalpiniaceae (Bénéluz, 2016). Therefore, since groups closely related to *Morpho*, notably the sister genus *Caerois*, are known to only feed on monocotyledon host-plants (Beccaloni *et al*., 2008), it is likely that the divergence of the *Morpho* was associated with an initial shift to dicotyledons. This host-plant shift at the root of Morphos created the conditions for an early rapid diversification of the group.

A shift towards the canopy driving phenotypic and diversification changes

We found a shift of species diversification associated with a single shift from the understory to the canopy (DeVries *et al.* 2010; Chazot *et al*. 2016). We also found strong indications that female wing shape evolution in the canopy clade is different from a neutral evolution. An increasing rate of shape evolution for both fore- and hind-wings was supported in the subclade nested in the canopy clade and including *M. theseus*, *M. niepelti*, *M. amphytrion*, *M. telemachus*, and *M. hercules*. Chazot *et al*. (2016) showed that both male and female wing shapes in the canopy clade are significantly different from wing shapes in understory species. Here we show that this microhabitat change associated with different vegetation structure, microclimatic conditions and predator community may have also affected the rate of female wing shape evolution in addition to shape *per se*. However, we note that the highest rate shift was not placed at the root of the canopy clade, suggesting that other factors may have caused this rapid phenotypic evolution. This increased rate of wing shape evolution was not found in males. Instead, in males we found two significant slowdowns in rate at different small subclades, only in the case of hindwings. The lack of more precise information on these species ecology unfortunately prevents speculating on the factors involved in such changes in wing shape evolutionary rate.

A second change in microhabitat conditions associated with a host-plant, phenotypical and diversification shifts

Published information in the *portis* clade (Heredia & Alvarez, 2007; Beccaloni *et al.*, 2008; Montero Abril & Ortiz Perez, 2010) indicate that four *Morpho* species (*M. portis, M. aega*, *M. sulkowskyi* and *M. rhodopteron*) feed on Neotropical woody bamboos (Poaceae, tribe Bambuseae), notably on *Chusquea* species (subtribe Chusqueinae), in particular *Chusquea* aff. *scandens* for *M. sulkowskyi* that occurs at cloud forest elevations (Heredia & Alvarez, 2007). Recent observations indicate that M. zephyritis also feeds on woody bamboos (Roberto Maravi, pers. comm.). For the other species of the *portis* clade, there are only field observations indicating that they live in areas with important bamboo vegetation (Purser & Lacomme, 2016; pers. obs. in Peru, Daniel Lacomme pers. com.).

If, as observations indicate, the *portis* clade diversified after an initial shift back to monocotyledon host-plants, this reversal evolutionary event is a strong support for the "oscillation hypothesis" (Janz *et al.*, 2006). This hypothesis was proposed to explain the pattern of nymphalid butterflies with respect to host-plant use (Janz *et al.*, 2006) and states that the ability to recolonize "lost" hosts should be conserved over long evolutionary times, leading to recurrent recolonization events. Compared to the speciation rate of the backbone, species diversification within the *portis* clade proceeded at a higher rate, and rapidly decreased through time to reach almost zero at present. Adaptive radiations, here following a major host-plant shift, predict this rapid dampening of speciation rate as a result of niche filling (Schluter, 2000; Gavrilets & Losos, 2009).

Interestingly, we found that an evolutionary jump – a fast punctuational event of evolution – toward smaller wing sizes also coincided with the host-plant shift. Chazot *et al*. (2016) did not identify any driver of this wing size evolution. To our knowledge, there is no

clear expectation or evidence supporting a specific relationship between body size and monocot *versus* dicot feeders but this question has rarely been addressed (but see Garcia-Barros 2000). The jump toward smaller sizes also cannot be associated with any altitudinal change because some species of the clade only occur at low to mid altitudes (200-1500 m), while others occur at higher altitudes (1500-3500 m) (Blandin, 2007; Gayman *et al*., 2016).

Therefore, other hypotheses need to be explored, in particular that of a second possible change of microhabitat conditions. Many Bambusinae, in particular *Chusquea* species, form dense thickets, twigs and leaves creating inextricable tangles as a result from abundant vegetative branching at each node (Fisher, 2011; Fisher *et al*., 2014). Observational data on the behaviour of the bamboo feeding *Morpho* is scarce, but observations on *M. rhodopteron* (Montero Abril and Ortiz Perez, 2010; Purser and Lacomme, 2016), *M. sulkowskyi* (Heredia and Alvarez-Lopez 2007), and *M. aega* (Otero & Marigo, 1990) suggest that females are more often resting inside the *Chusquea* thickets while males are flying around (males, when resting, also stand in the vegetation). Moreover, Heredia & Alvarez-Lopez (2007) noted that *M. sulkowskyi* females having light and dark alternating stripes on wings ventral side are difficult to detect inside *Chusquea* thickets. More or less contrasted similar patterns exist in males and females of other species, except in *M. absoloni*. Therefore, we hypothesize that size reduction, associated to a more or less striped appearance of the ventral side, could be an adaptation to the microhabitat structure of dense woody bamboo thickets, highlighting once again the importance of the microhabitat conditions on species and trait evolution.

Declining diversity in the Neotropical Morpho

When accounting for heterogeneity in diversification rates (isolating the two shifting subclades), the diversification dynamics for the remaining lineages was characterized by a

554 negative net diversification rate, indicative of a declining diversity, mainly during the
555 Miocene. Whether diversity decline can be accurately estimated only from phylogenies of
556 extant species is a matter of debate (e.g. Quental & Marshall, 2010; but see Morlon *et al.*,
557 2011). In the case of *Morpho*, this pattern may explain why some branches in the tree (such
558 as the stem branch of *M. marcus* and *M. eugenia* or the branches leading to *M. anaxibia*, *M.*
559 *deidamia*, or *M. polyphemus*) are surprisingly long. Extinct lineages may also explain why *M.*
560 *polyphemus*, which diverged from its sister clade 20 Ma, is found in Central America, while
561 colonization of Central America is often expected to be much more recent (but see Montes *et*
562 *al.*, 2015, Farris *et al*., 2011). Major landscape transformations during the Miocene in western
563 Amazonia may explain this decline. Between 23-10 Ma, Western Amazonia transformed into
564 a large wetland of lakes, swamps and shallow water, called the Pebas System (Wesselingh
565 *et al.*, 2001; Hoorn *et al.*, 2010). The exact nature of the Pebas System is still under
566 discussion but it was most likely unsuitable for terrestrial fauna (Salas-Gismondi *et al.*,
567 2015). Evidence of extinction has been found from a west Amazonian fossil record, in
568 particular with a major decrease of mammalian diversity at the transition between the
569 Oligocene and the Miocene (Antoine *et al*., 2016), which is in line with the beginning of the
570 diversity decline in *Morpho* (Fig. 3).
571
572 *Conclusion*
573 Our results support a prevailing ecological basis for both species and phenotypic
574 diversification in *Morpho* butterflies: (1) a major host-plant shift, which affected wing size
575 evolution and greatly affected species diversification dynamics (pattern of adaptive
576 radiation), and (2) a microhabitat shift affecting species diversification and partially wing
577 shape diversification. Therefore, to a large extent, the dynamics of species diversification and
578 phenotypic diversification are coupled in *Morpho*, most likely as a result of two major

ecological events. More importantly, we show that both species and phenotypic diversification in *Morpho* butterflies are better explained by multiple clade-specific factors instead of global abiotic drivers. Current methods for identifying drivers of diversification, based on model comparisons, are unable to test for potential interactions between drivers. Hence, our results do not exclude the possibility that the Andes played a role in diversification, but rather suggest that their effect on the shape of the phylogenetic tree was less significant than other factors. Nevertheless, the extent to which the effects of these ecological drivers can be generalised is unknown given the scale of our dataset. In particular future work at a larger phylogenetic scale should shed light on the importance of major host-plant transitions on the evolution of body size and the dynamics of diversification. Our study also highlights that both phenotypic and ecological information are of key relevance for understanding macroevolutionary patterns of diversification.

Table 1. Summary results obtained from fitting three models of trait evolution on 100 trees, using the *rjmcmc.bm* function as implemented in the R package GEIGER on a) males and b) females. *bm*=single Brownian rate, *rbm*=relaxed Brownian rates, *jbm*=jumps of Brownian rates. AICbm, AICrbm, AICjbm = mean AIC score across the 100 trees for all three models. ΔAIC bm-rbm, ΔAIC bm-jbm, ΔAIC rbm-jbm = pairwise AIC differences between models for each tree.

a) Males

	AICbm	AICrbm	AICjbm	ΔAIC bm-rbm	ΔAIC bm-jbm	ΔAIC rbm-jbm
Forewing	-23.92 (18.72)	-27.78 (10.33)	13.41 (26.32)	3.85 (21.70)	-37.34 (34.54)	-41.20 (30.02)
Hindwing	-14.43 (20.28)	-18.62 (14.58)	14.94 (24.28)	4.18 (24.02)	-29.37 (29.76)	-33.56 (28.21)

b) Females

	AICbm	AICrbm	AICjbm	ΔAIC bm-rbm	ΔAIC bm-jbm	ΔAIC rbm-jbm
Forewing	-22.36 (10.44)	-17.74 (9.40)	-34.70 (1.60)	-4.61 (15.73)	12.33 (10.98)	16.95 (9.56)
Hindwing	-15.44 (17.06)	-13.30 (22.83)	-32.80 (1.17)	-2.14 (29.62)	17.36 (16.88)	19.50 (23.01)

603 **Table 2.** Paleoenvironmental-dependent diversification analyses using paleoaltitude (a) and
604 Cenozoic temperature (b) data. Mean parameter and standard error estimates are presented
605 for each model. Best-fitting model, as determined via a combination of the lowest AIC and
606 ΔAIC (see main text) highlighted in bold. In our best-fit paleoaltitude-dependent model,
607 speciation is negatively correlated to Andean orogeny over time (adding extinction as a
608 parameter did not improve the model fit). Likewise, speciation is positively correlated to
609 temperature variation over time (allowing extinction to vary with temperature did not
610 improve the likelihood). λ = speciation rate (in events/Myr/lineage); μ = extinction rate (in
611 events/Myr/lineage); α = rate of variation of the speciation according to the relevant
612 paleoenvironmental variable; β = rate of variation of the extinction according to the
613 paleoenvironmental variable; NP = number of parameters in each model.

614
615
616 **a) Paleoaltitude models**
617

Models	Dependency	NP	logL	AIC	ΔAIC	λ	α	μ	β
λ Alti. and no μ	Linear	2	-97.50 ±0.085	199.00 ±0.171	0.00	0.190 ±0.004	-3.60E-05 ±1.39E-06	-	-
λ Alti. and no μ	Exponential	2	-97.68 ±0.083	199.37 ±0.166	0.37	0.210 ±0.004	-3.06E-04 ±5.76E-06	-	-
λ Alti and μ constant.	Linear	3	-97.49 ±0.085	200.99 ±0.170	1.99	0.190 ±0.0003	-3.47E-05 ±8.75E-07	5.15E-04 ±4.17E-04	-
λ Alti. and μ constant	Exponential	3	-97.69 ±0.083	201.37 ±0.166	2.37	0.220 ±0.004	-3.11E-04 ±5.68E-06	9.09E-07 ±7.91E-07	-
λ constant and μ Alti	Exponential	3	-97.75 ±0.104	201.51 ± 0.207	2.51	0.080 ±3.16E-04	-	42038.92 ±11873.33	-7.48E-03 ±2.62E-04
λ Alti. and μ Alti	Exponential	4	-96.94 ±0.094	201.87 ±0.187	2.87	0.880 ±0.160	-5.00E-04 ±2.00E-05	6.820 ±1.159	-1.89E-03 ±4.72E-05
λ Alti. and μ Alti.	Linear	4	-97.42 ±0.086	202.83 ±0.171	3.84	0.210 ±0.004	-3.83E-05 ±1.18E-06	0.070 ±0.007	-2.38E-05 ±2.32E-06
λ constant and μ Alti.	Linear	3	-98.56 ±0.099	203.12 ±0.198	4.12	0.080 ±0.001	-	0.030 ±0.005	-1.14E-05 ±1.76E-06

618

b) Paleoclimate models

Models	Dependency	NP	logL	AIC	ΔAIC	λ	α	μ	β
λ Temp. and no μ	Exponential	2	-96.65 ±0.095	197.30 ±0.189	0.00	0.030 ±4.13E-04	0.179 ±1.91E-03	-	-
λ Temp. and no μ	Linear	2	-96.72 ±0.097	197.44 ±0.195	0.13	0.015 ±5.50E-04	0.013 ±1.17E-04	-	-
λ Temp and μ constant	Exponential	3	-96.58 ±0.092	199.15 ±0.184	1.85	0.030 ±3.93E-04	0.210 ±3.62E-03	0.043 ±0.004	-
λ Temp. and μ constant	Linear	3	-96.67 ±0.097	199.33 ±0.195	2.03	0.023 ±1.48E-03	0.021 ±1.34E-03	0.046 ±0.007	-
λ Temp. and μ Temp.	Linear	4	-96.42 ±0.095	200.85 ±0.189	3.54	0.017 ±1.11E-03	0.027 ±8.07E-04	0.290 ±0.012	-0.037 ±0.002
λ Temp. and μ Temp	Exponential	4	-96.55 ±0.092	201.10 ±0.183	3.80	0.032 ±7.99E-04	0.205 ±4.57E-03	0.156 ±0.040	-0.164 ±0.019
λ constant and μ Temp.	Exponential	3	-98.57 ±0.103	203.14 ±0.205	5.84	0.081 ±2.96E-04	-	4.47E-08 ±3.08E-09	0.004 ±2.19E-04
λ constant and μ Temp.	Linear	3	-98.57 ±0.103	203.14 ±0.205	5.84	0.081 ±2.97E-04	-	1.09E-04 ±1.08E-04	-1.37E-05 ±1.37E-05

623 **Table 3.** Results of model comparison for the five time-dependent diversification analyses
624 presented, with mean parameter estimates for each model. λ = speciation rate (in
625 events/Myr/lineage); α = parameter of rate variation for speciation; μ = extinction rate (in
626 events/Myr/lineage); β = parameter of rate variation for extinction; NP = number of
627 parameters in each model; AICc = corrected Akaike information criterion; logL = log-
628 likelihood.
629

Clade partition	Models	NP	logL	AIC	λ	α	μ	β	Joint logL	Joint AIC
background	BVAR DVAR	4	-35.68	79.36	0.063	0.237	0.079	0.228		
monocots	BVAR	2	-21.78	47.55	0.014	0.213	-	-	-88.84	191.69
canopy	BCST	1	-31.39	64.77	0.083	-	-	-		
background	BCST	1	-50.91	103.83	0.072	-	-	-		
monocots	BVAR	2	-21.78	47.55	0.014	0.213	-	-	-92.83	193.66
shape shift	BCST	1	-20.14	42.28	0.095	-	-	-		
background	BCST	1	-73.75	149.49	0.081	-	-	-	-95.52	197.05
monocots	BVAR	2	-21.78	47.55	0.014	0.213	-	-		
whole	BCST	1	-98.40	198.81	0.081	-	-	-	-98.40	198.81
background	BCST	1	-78.18	158.36	0.078	-	-	-	-98.32	200.63
shape shift	BCST	1	-20.14	42.28	0.095	-	-	-		
background	BCST	1	-67.01	136.03	0.080	-	-	-	-98.40	200.80
canopy	BCST	1	-31.39	64.77	0.083	-	-	-		

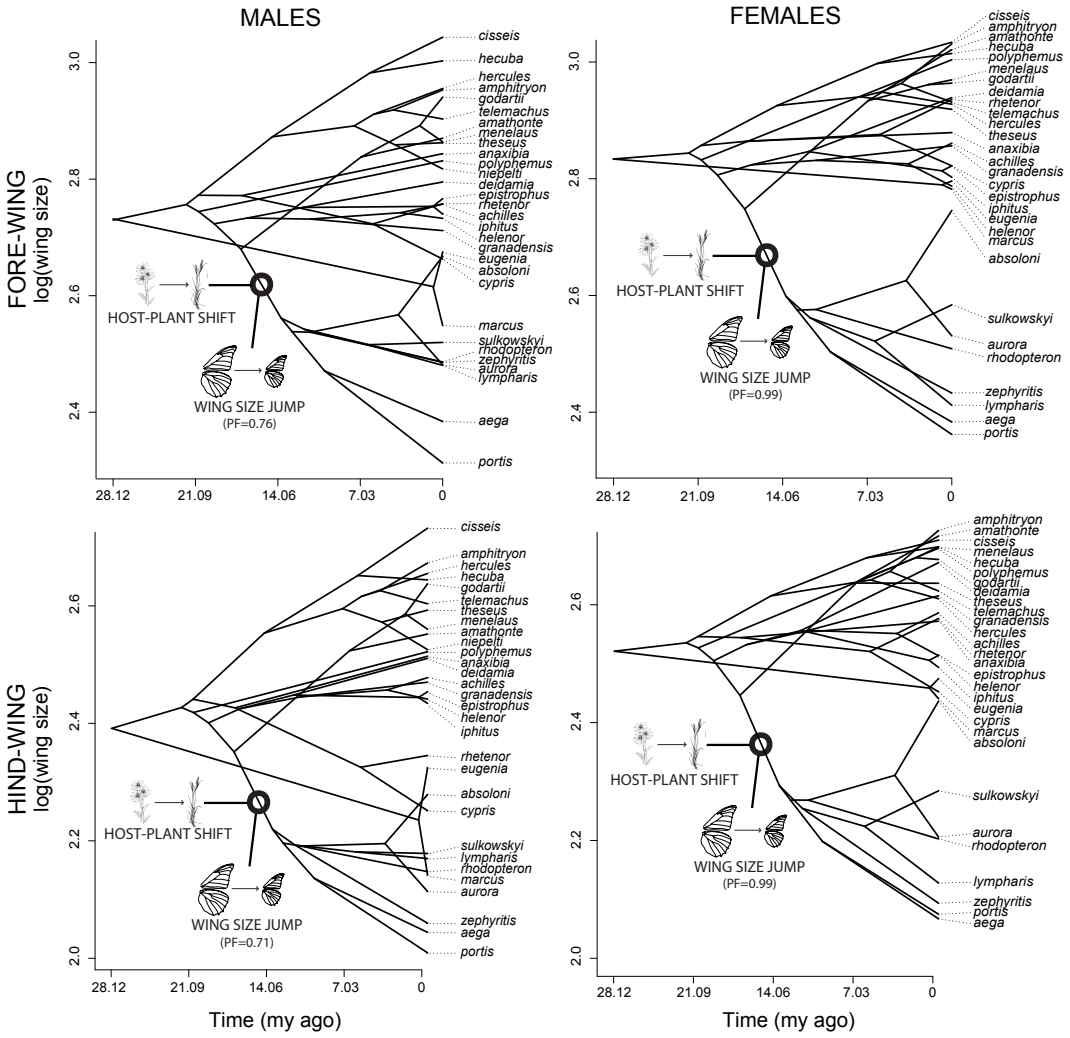

Figure 1. Phenograms for wing size (log scale) for males (left panels) and females (right panels). The top panels are the forewings, and the bottom panels are the hindwings. Wing size values are reconstructed at the nodes and plotted on a time scale. Phylogenetic relationships are projected into the phenogram. The position (branch) where the main host-plant shift and significant wing size jump happened is also shown. PF values indicate the frequency at which each jump was found across the posterior distribution of trees.

a) Males

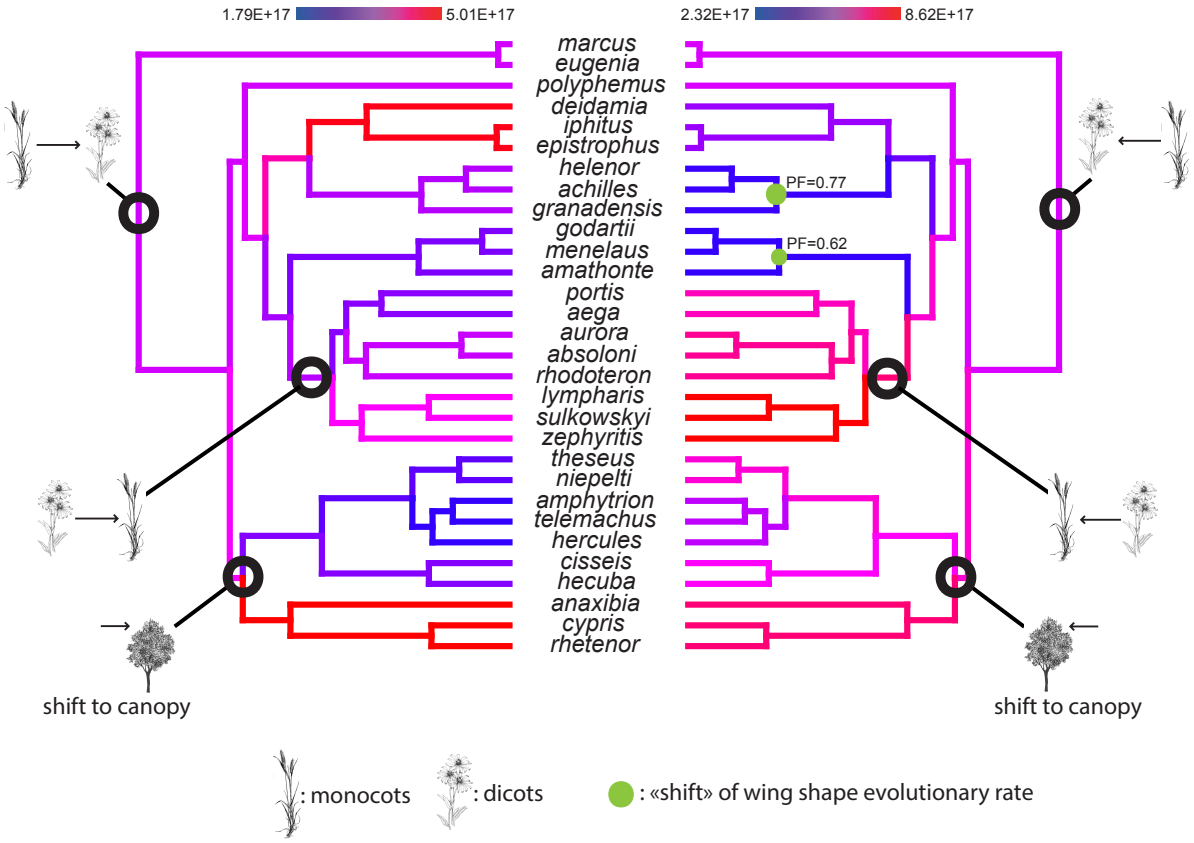

b) Females

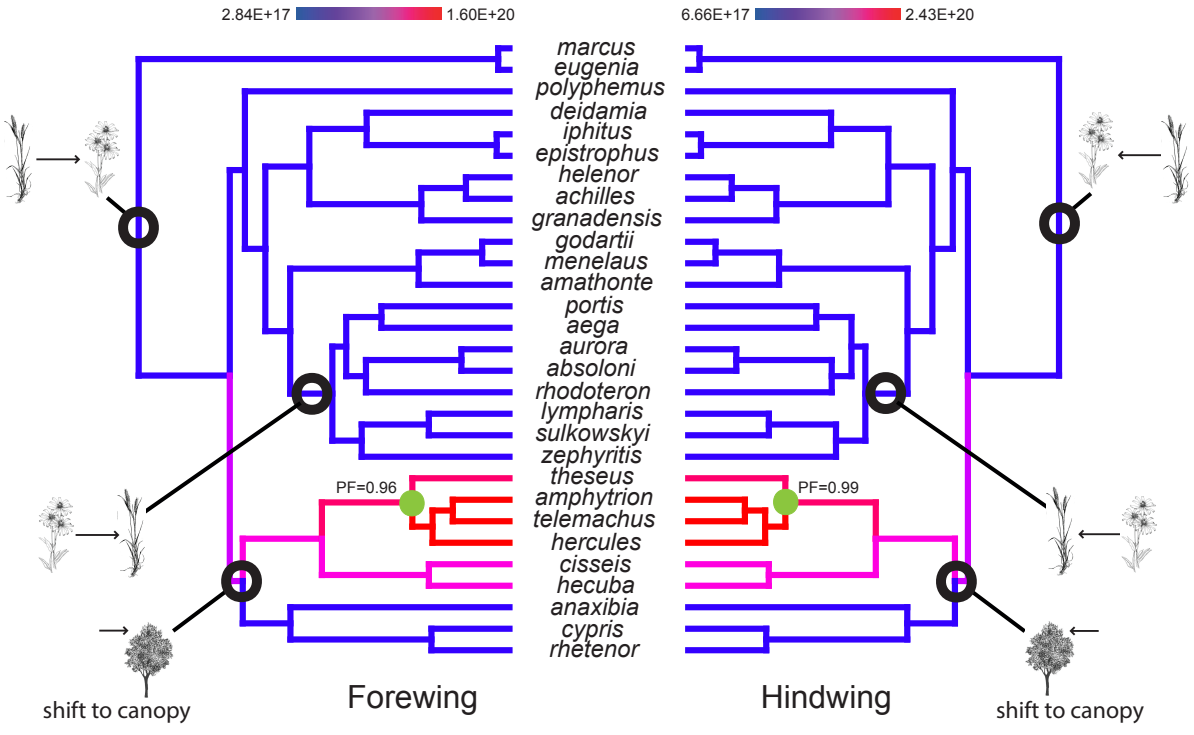

Figure 2. Rate of wing shape diversification for a) males and b) females. Branches of the phylogenies are coloured according to the evolutionary rate inferred at the nodes using the R package GEOMORPH. Green points indicate the changes in the rate of wing shape evolution and black points the evolutionary jumps of wing size. Only shifts with a posterior tree frequency higher than 0.5 are shown. PF values indicate the frequency at which each shift was found across the posterior distribution of trees. On these phylogenies some major evolutionary events including important host-plant shifts and microhabitat shifts are also indicated.

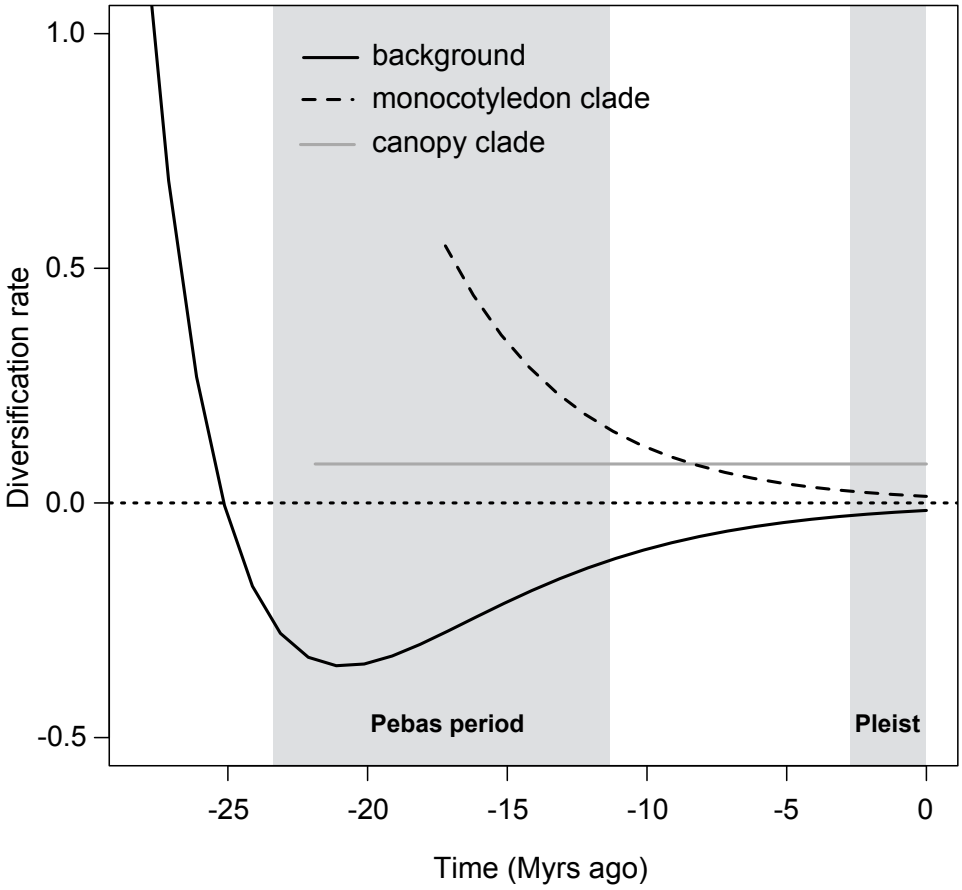
1.0
0.5
0.0
-0.5
Diversification rate
background
monocotyledon clade
canopy clade
Pebas period
Pleist
-25
-20
-15
-10
-5
0
Time (Myrs ago)

650 **Figure 3.** Estimation of the temporal dynamics of diversification for the genus *Morpho*.
651 Diversification rates (speciation minus extinction) for the best models identified for the
652 different subclades (canopy and monocotyledon) and the remaining lineages (background).
653 The early background diversification is elevated and decreases through time until it becomes
654 negative in the early Miocene. The canopy clade has constant rates of diversification, while
655 the monocotyledon clade conforms to an early-burst pattern with high rates that decrease
656 toward the present.
657

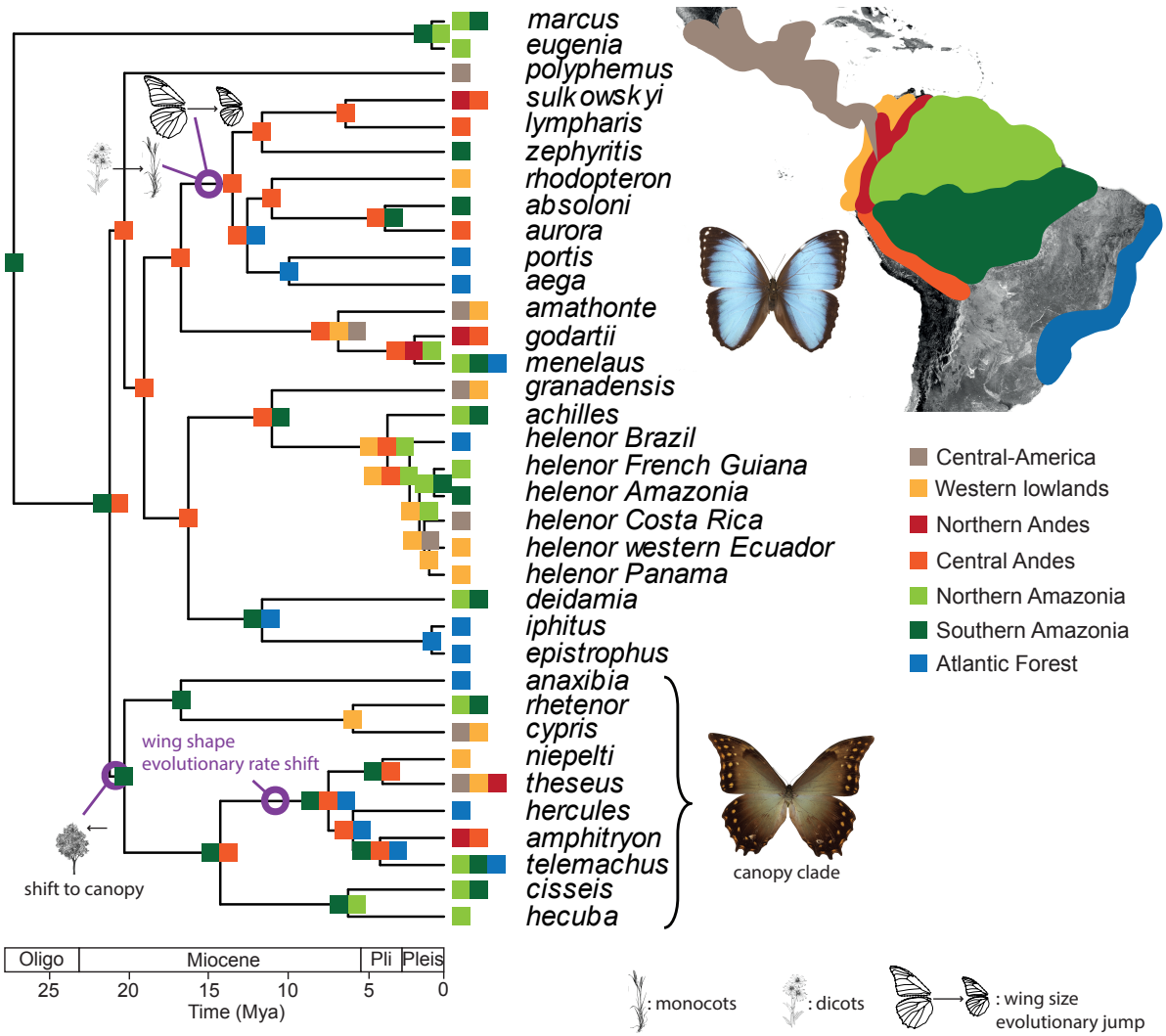

Figure 4. Historical biogeography inferred for the genus *Morpho*. The most likely states are indicated at the nodes. The different clade-specific ecological factors are also indicated on the tree. The two pictures of *Morpho* depict the typical wing shapes associated with each microhabitat – top: short rounded wings characteristic of the understory species, bottom: elongated wings toward the apex characteristic of the canopy clade.

665 **REFERENCES**

666 Adams D.C. (2014). Quantifying and comparing phylogenetic evolutionary rates for shape and other
667 high-dimensional phenotypic data. *Systematic Biology*, 63, 166-177.

668 Antoine P.O., Abello M.A., Adnet S., Sierra A.J.A., Baby P., Billet G., Corfu F., … and R. Salas-
669 Gismondi (2016). A 60-million-year Cenozoic history of western Amazonian ecosystems in
670 Contamana, eastern Peru. *Gondwana Research* 31, 30-59.

671 Beaulieu J.M. and B.C. O'Meara. (2015). Extinction can be estimated from moderately sized
672 molecular phylogenies. *Evolution*, 69, 1036-1043.

673 Beccaloni G.W., Viloria A.L., Hall S.K., and G.S. Robinson (2008). Catalogue of the hostplants of the
674 Neotropical butterflies. Sociedad Entomológica Aragonesa. Monografias Tercer Milenio, 8, 1-
675 536.

676 Blandin P. (2007). The systematics of the genus *Morpho* Fabricius, 1807. Hillside Books, Canterbury.

677 Blandin P. and B. Purser (2013). Evolution and diversification of Neotropical butterflies: Insights
678 from the biogeography and phylogeny of the genus *Morpho* Fabricius, 1807 (Nymphalidae:
679 Morphinae), with a review of the geodynamics of South America. *Tropical Lepidoptera*
680 *Research*, 23, 62-85.

681 Cassildé C., Blandin P., Pierre J. and T. Bourgoin (2010). Phylogeny of the genus *Morpho* Fabricius,
682 1807, revisited (Lepidoptera, Nymphalidae). *Bulletin de la Société Entomologique de France*,
683 115, 225-250.

684 Cassildé C., Blandin P. and J.F. Silvain (2012). Phylogeny of the genus *Morpho* Fabricius 1807:
685 insights from two mitochondrial genes (Lepidoptera: Nymphalidae). *Annales de la Société*
686 *Entomologique de France*, 48, 173-188.

687 Chazot N., Panara S., Zilbermann N., Blandin P., Le Poul Y., Cornette R., Elias M. and V. Debat
688 (2016). Morpho morphometrics: Shared ancestry and selection drive the evolution of wing size
689 and shape in Morpho butterflies. *Evolution*, 70, 181-194.

690 Chazot N., Willmott K.R., de-Silva D.L., Condamine F., Morlon H., Freitas A.V.L., Uribe S.,
691 Giraldo-Sanchez C., Lamas G., Joron M., Jiggins C. and M. Elias (2016). Into the Andes:

692 Multiple colonisations and local diversification explain Andean diversity in the Godyridina
693 butterfly subtribe (Ithomiini). *Molecular Ecology*, 25, 5765-5784.
694 Chazot N., Willmott K.R., Lamas G., Freitas A.V.L., Piron-Prunier F., Arias C.F., De-Silva D.L. and
695 M. Elias (2018). Renewed diversification following Miocene landscape turnover in a
696 Neotropical butterfly radiation. Global Ecology and Biogeography, 28, 1118-1132.
697 Condamine F.L., Rolland J. and H. Morlon (2013). Macroevolutionary perspectives to environmental
698 change. *Ecology Letters*, 16, 72-85.
699 Condamine F.L., Antonelli A., Lagomarsino L.P., Hoorn C. and Liow L.H. (2018). Teasing apart
700 mountain uplift, climate change and biotic drivers of species diversification. In: Mountains,
701 Climate and Biodiversity (eds. Hoorn C., Perrigo A.L. & Antonelli A.). pp. 257-272. John
702 Wiley & Sons Ltd.
703 Constantino L.M. (1997). Natural history, immature stages and hostplants of *Morpho amathonte* from
704 western Colombia. *Tropical Lepidoptera*, 8, 75-80.
705 Cooney C. R. and Thomas G. H. (2021). Heterogeneous relationships between rates of speciation and
706 body size evolution across vertebrate clades. *Nature Ecology & Evolution*, 5, 101-110.
707 Denton J.S. and D.C. Adams (2015). A new phylogenetic test for comparing multiple
708 high-dimensional evolutionary rates suggests interplay of evolutionary rates and modularity in
709 lanternfishes (Myctophiformes; Myctophidae). *Evolution*, 69, 2425-2440.
710 De-Silva D.L., Elias M., Willmott K., Mallet J. and J.J. Day (2016). Diversification of clearwing
711 butterflies with the rise of the Andes. *Journal of Biogeography*, 43, 44-58.
712 De-Silva D.L., Mota L.L., Chazot N., Mallarino R., Silva-Brandão K.L., Piñerez L.M.G., Freitas
713 A.V.L., Lamas G., Joron M., Mallet J., Giraldo C.E., Uribe S., Särkinen T., Knapp S., Jiggins
714 C.D., Willmott K.R. and M. Elias (2017). Origin and diversification of the largest ithomiine
715 butterfly genus, *Pteronymia* Butler & Druce, 1872 (Lepidoptera: Nymphalidae), in the Northern
716 Andes. *Scientific Reports*, 7, 45966.
717 DeVries P.J., Penz C.M. and R.I. Hill (2010). Vertical distribution, flight behaviour and evolution of
718 wing morphology in *Morpho* butterflies. *J Anim Ecol*, 79, 1077-1085.

719 Drummond A.J., Suchard M.A., Xie D. and A. Rambaut (2012). Bayesian phylogenetics with BEAUti
720 and the BEAST 1.7. *Molecular Biology and Evolution*, 29, 1969-1973.
721 Dudley R. (2002). *The biomechanics of insect flight*. Princeton Univ. Press, Princeton, NJ.
722 Eastman J.M., Alfaro M.E., Joyce P., Hipp A.L. and L.J. Harmon (2011). A novel comparative
723 method for identifying shifts in the rate of character evolution on trees. *Evolution*, 65, 3578-
724 3589.
725 Elias M., Joron, M., Willmott K., Silva-Brandão K.L., Kaiser V., Arias C.F., Gomez Piñeres L.M.,
726 Uribe S., Brower A.V.Z., Freitas A.V.L. and C. Jiggins (2009). Out of the Andes: patterns of
727 diversification in clearwing butterflies. *Molecular Ecology*, 18, 1716-1729.
728 Evenstar L.A., Stuart F.L., Hartley A.J. and B. Tattitch (2015). Slow Cenozoic uplift of the western
729 Andean Cordillera indicated by cosmogenic ^{3}He in alluvial boulders from the Pacific Planation
730 Surface. *Geophysical Research Letter*, 42, 8448-8455.
731 Farris D.W., Jaramillo C. Bayona G., Restrepo-Moreno S.A., Montes C., Cardona A., Mora A.,
732 Speakman R.J., Glascock M.D. and V. Valencia (2011). Fracturing of the Panamanian Isthmus
733 during initial collision with South-America. *Geology*, 39, 1007-1010.
734 Fiorella R.P., Poulsen C.J., Pillco Zolá R.S., Barnes J.B., Tabor C.R. and T.A. Ehlers (2015).
735 Spatiotemporal variability of modern precipitation δ^{18}O in the central Andes and implications
736 for paleoclimate and paleoaltimetry estimates. *Journal of Geophysical Research: Atmospheres*,
737 120, 4630-4656.
738 Foote M. (1997). The evolution of morphological diversity. *Annual Review of Ecology and*
739 *Systematics*, 28, 129-152.
740 García-Barros E. (2000). Body size, egg size, and their interspecific relationships with ecological and
741 life history traits in butterflies (Lepidoptera: Papilionoidea, Hesperioidea). *Biological Journal*
742 *of the Linnean Society*, 70, 251-284.
743 Gavrilets S. and J. B. Losos (2009). Adaptive radiation: contrasting theory with data. *Science*, 323,
744 732-737.
745 Grodnitsky D.L., Dudley R. and L. Gilbert (1994). Wing decoupling in hovering flight of swallowtail
746 butterflies (Lepidoptera: Papilionidae). *Tropical Lepidoptera*, 5, 85-86.

747 Harmon L.J., Weir J., Brock C., Glor R.E. and W. Challenger (2008). GEIGER: Investigating
748 evolutionary radiations. *Bioinformatics,* 24, 129-131.
749 Hoorn C., Wesselingh F.P., ter Steege H., Bermudez M.A., Mora A., Sevink J., Sanmartín I.,
750 Sanchez-Meseguer A., Anderson C.L., Figueiredo J.P., Jaramillo C., Riff D., Negri F.R.,
751 Hooghiemstra H., Lundberg J., Stadler T., Sarkinen T. and A. Antonelli (2010). Amazonia
752 through time: andean uplift, climate change, landscape evolution, and biodiversity. *Science,*
753 330, 927-931.
754 Janz N., Nylin S. and N. Wahlberg (2006). Diversity begets diversity: host expansions and the
755 diversification of plant-feeding insects. *BMC Evolutionary Biology*, 6, 4.
756 Lagomarsino L.P., Condamine F.L., Antonelli A., Mulch A. and C.C. Davis (2016). The abiotic and
757 biotic drivers of rapid diversification in Andean bellflowers (Campanulaceae). *New Phytologist*,
758 210, 1430-1442.
759 Lanfear R., Calcott B., Ho S.Y.W. and S. Guindon (2012). PartitionFinder: combined selection of
760 partitioning schemes and substitution models for phylogenetic analyses. *Molecular Biology and*
761 *Evolution*, 29, 1695-1701.
762 Langerhans R.B., Anderson C. M. and J. L. Heinen-Kay (2016). Causes and consequences of genital
763 evolution. *Integrative and Comparative Biology*, 56, 741-751.
764 Lee M.S., Sanders K.L., King B. and A. Palci (2016). Diversification rates and phenotypic evolution
765 in venomous snakes (Elapidae). *Royal Society Open Science*, 3, 150.
766 Leier A., McQuarrie N., Garzione C. and J. Eiler (2013). Stable isotope evidence for multiple pulses
767 of rapid surface uplift in the Central Andes, Bolivia. *Earth and Planetary Science Letters*, 371,
768 49-58.
769 Le Roy C., Cornette R., Llaurens V. and Debat V. (2019). Effects of natural wing damage on flight
770 performance in Morpho butterflies: what can it tell us about wing shape evolution? *Journal of*
771 *Experimental Biology*, 222, xxx-yyy.
772 Le Roy C., Debat V. and Llaurens, V. (2019). Adaptive evolution of butterfly wing shape: from
773 morphology to behaviour. *Biological Reviews*, 94, 1261-1281.

774 Matzke N.J. (2014). Model selection in historical biogeography reveals that founder-event speciation
775 is a crucial process in island clades. *Systematic Biology*, 63, 951-970.
776 Merrill R.M., Chia A. and N.J. Nadeau (2014). Divergent warning patterns contribute to assortative
777 mating between incipient *Heliconius* species. *Ecology & Evolution*, 4, 911–917.
778 Montes C., Cardona A., McFadden R., Morón S.E., Silva C.A., Restrepo-Moreno S., Ramírez D.A.,
779 Hoyos N., Wilson J., Farris D., Bayona G.A., Jamarillo C.A., Valencia V., J. Bryan and J.A.
780 Flores (2012). Evidence for middle Eocene and younger land emergence in central Panama:
781 implications for Isthmus closure. *Geol Soc Am Bull*, 124, 780-799.
782 Morlon H., Parsons T.L. and J.B. Plotkin (2011). Reconciling molecular phylogenies with the fossil
783 record. *Proceedings of the National Academy of Sciences of the U.S.A.*, 108, 16327-16332.
784 Naisbit R.E., Jiggins C.D. and J. Mallet (2001). Disruptive sexual selection against hybrids
785 contributes to speciation between *Heliconius cydno* and *Heliconius melpomene*. *Proceedings of*
786 *the Royal Society of London B: Biological Sciences*, 268, 1849-1854.
787 Ortiz-Acevedo E., Gomez J. P., Espeland M., Toussaint, E. F. and Willmott K. R. (2020). The roles of
788 wing color pattern and geography in the evolution of Neotropical Preponini butterflies. *Ecology*
789 *and Evolution*, 10, 12801-12816.
790 Plummer M., Best N., Vines K., Sarkar D., Bates D., Almond R., Magnusson A. (2020). coda:
791 Output Analysis and Diagnostics for MCMC. R CRAN respository, https://cran.r-
792 project.org/web/packages/coda/index.html
793 Penz C.M., Devries P.J. and N. Wahlberg (2012). Diversification of Morpho butterflies (Lepidoptera,
794 Nymphalidae): a re-evaluation of morphological characters and new insight from DNA
795 sequence data. *Systematic Entomology*, 37, 670-685.
796 Price S.A., Claverie T., Near T.J. and P.C. Wainwright (2015). Phylogenetic insights into the history
797 and diversification of fishes on reefs. *Coral Reefs*, 34, 997-1009.
798 Quental, T. B. and Marshall, C. R. (2010). Diversity dynamics: molecular phylogenies need the fossil
799 record. *Trends in Ecology & Evolution*, 25, 434-441.
800 Rabosky D.L. (2010). Extinction rates should not be estimated from molecular phylogenies.
801 *Evolution*, 64, 1816-1824.
802 Rabosky D.L. and Adams DC. (2012). Rates of morphological evolution are correlated with species
803 richness in salamanders. *Evolution,* 66, 1807-1818.

804 Rabosky D.L., Santini F., Eastman J.M., Smith S.A., Sidlauskas B., Chang J. and Alfaro M.E. (2013).
805 Rates of speciation and morphological evolution are correlated across the largest vertebrate
806 radiation. *Nature Communications*, 4, 2958.
807 Rabosky R.D., Donnellan S.C., Grundler M. and I. Lovette (2014). Analysis and visualization of
808 complex macroevolutionary dynamics: an example from Australian scincid lizards. *Systematic*
809 *Biology*, 63, 610-627.
810 Ree R.H. and S.A. Smith (2008) Maximum likelihood inference of geographic range evolution by
811 dispersal, local extinction, and cladogenesis. *Systematic Biology,* 57, 4-14.
812 Revell L.J. (2012) phytools: An R package for phylogenetic comparative biology (and other things).
813 *Methods in Ecology & Evolution*, 3, 217-223.
814 Salas-Gismondi R., Flynn J.J., Baby P., Tejada-Lara J.V., Wesselingh F.P. and P.O. Antoine (2015).
815 A Miocene hyperdiverse crocodylian community reveals peculiar trophic dynamics in proto-
816 Amazonian mega-wetlands. *Proceedings of the Royal Society of London B: Biological*
817 *Sciences*, 282, 20142490.
818 Sauquet H., Ho S.Y., Gandolfo M.A., Jordan G.J., Wilf P., Cantrill D.J., Bayly M.J., Bromham L.,
819 Brown G.K., Carpenter R.J., Lee D.M., Murphy D.J., Sniderman J.M. and F. Udovicic (2011).
820 Testing the impact of calibration on molecular divergence times using a fossil-rich group: the
821 case of *Nothofagus* (Fagales). *Systematic Biology*, 61, 289-313.
822 Schluter D. (2000). *Ecology of adaptive radiation.* Oxford: Oxford University Press.
823 Thacker C.E. (2014). Species and shape diversification are inversely correlated among gobies and
824 cardinalfishes (Teleostei: Gobiiformes). *Org Divers Evol*, 14, 419-436.
825 Uyeda J.C., Caetano D.S. and M.W. Pennell (2014). Comparative analysis of principal components
826 can be misleading. *Systematic Biology*, 64, 677-689.
827 Vásquez Bardales J., Zárate Gómez R., Huiñapi Canaquiri P., Pinedo Jiménez J., Ramírez Hernández
828 J. J., Lamas G., and Vela García P. (2017). Plantas alimenticias de 19 especies de mariposas
829 diurnas (Lepidoptera) en Loreto, Perú. *Revista peruana de biología*, 24(1), 35-42.
830 Venditti C., Meade A. and M. Pagel (2011). Multiple routes to mammalian diversity. *Nature*, 479,
831 393-396.

Wahlberg N., Leneveu J., Kodandaramaiah U., Peña C., Nylin S., Freitas A.V.L. and A.V.Z. Brower (2009). Nymphalid butterflies diversify following near demise at the Cretaceous/Tertiary boundary. *Proceedings of the Royal Society of London B: Biological Sciences*, 276, 4295-4302.

Wesselingh F.P., Räsänen M.E., Irion G., Vonhof H.B., Kaandorp R., Renema W., Romero Pittman L. and M. Gingras (2001). Lake Pebas: a palaeoecological reconstruction of a Miocene, long-lived lake complex in western Amazonia. *Cainozoic Research*, 1, 35-68.

Zachos J.C., Dickens G.R. and R.E. Zeebe (2008). An early Cenozoic perspective on greenhouse warming and carbon-cycle dynamics. *Nature*, 451, 279-283.

Zelditch M.L., Li J., Tran L.A. and D.L. Swiderski (2015). Relationships of diversity, disparity, and their evolutionary rates in squirrels (Sciuridae). *Evolution*, 69, 1284-1300.

Supporting Information S1: Tree reconstructed and time-calibrated using BEAST. Node ages in red and the 95% HPD bars are indicated at the nodes. Grey numbers from 1 to 7 are the positions of the different time-constraints used. We used uniform distributions bounded by the 95% HPD inferred by Wahlberg et al. (2009). Upper and lower boundaries are indicated. In green are the node numbers corresponding to the tests for different wing shape evolutionary rates.

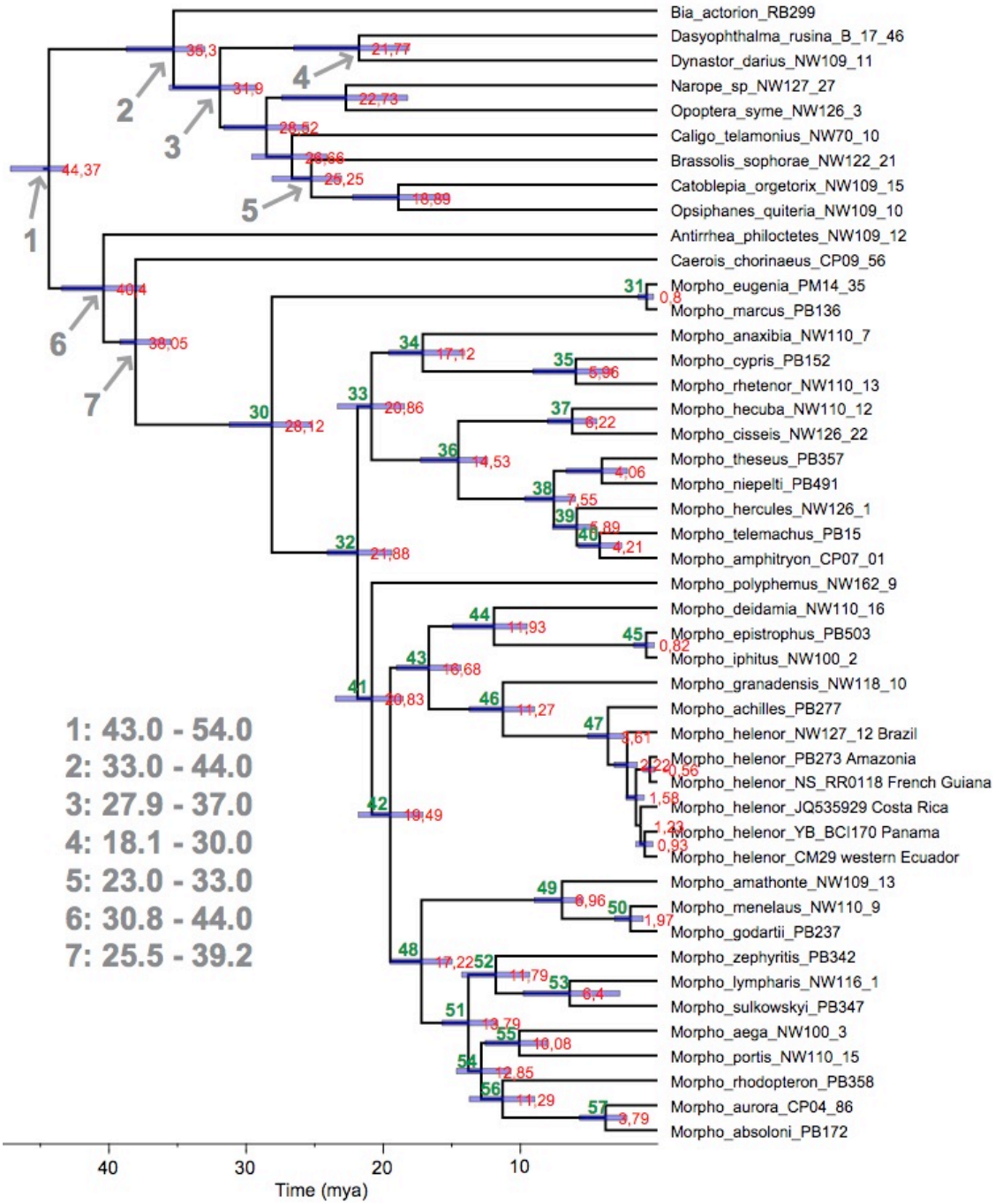

Supporting Information S2. Model comparison for wing size evolution for males and females for the analyses performed on the MCC tree.

a) Males

	Models	AIC	ΔAIC
Forewing	bm	126.833	0
	rbm	128.402	1.568
	jbm	153.859	27.025
Hindwing	bm	113.605	0
	rbm	115.105	1.5
	jbm	124.984	11.379

b) Females

	Models	AIC	ΔAIC
Forewing	jbm	122.68	0
	bm	154.069	31.389
	rbm	197.752	75.072
Hindwing	jbm	107.923	0
	rbm	117.123	9.2
	bm	197.547	89.624

Supporting Information S3. A. Results of models with shifts in rates of wing shape evolution for males on the MCC tree.

a) One-shift models

Wing	Node	Ingroup rate	Background rate	Ratio	p-value
Forewing	33	3.11E+17	3.70E+17	1.18	0.962
	34	5.01E+17	3.34E+17	1.50	0.927
	36	2.30E+17	3.87E+17	1.68	0.505
	38	2.05E+17	3.80E+17	1.85	0.228
	39	1.79E+17	3.70E+17	2.06	0.294
	42	2.92E+17	4.38E+17	1.49	0.452
	43	3.03E+17	4.13E+17	1.36	0.451
	44	2.62E+17	4.02E+17	1.53	0.846
	45	2.77E+17	3.77E+17	1.36	0.978
	46	3.19E+17	3.54E+17	1.11	0.985
	48	2.52E+17	3.70E+17	1.47	0.918
	49	2.93E+17	3.57E+17	1.21	0.933
	52	2.22E+17	3.65E+17	1.64	0.332
	54	3.78E+17	3.44E+17	1.09	0.912
	55	2.69E+17	3.60E+17	1.33	0.414
	57	4.87E+17	3.35E+17	1.45	0.672
Hindwing	33	5.6627E+17	5.4632E+17	1.03	0.994
	34	7.0283E+17	5.3632E+17	1.31	0.974
	36	5.0774E+17	5.6674E+17	1.11	0.93
	38	5.5832E+17	5.519E+17	1.01	0.984
	39	4.2922E+17	5.6672E+17	1.32	0.751
	42	4.7833E+17	6.6492E+17	1.39	0.536
	43	4.9549E+17	6.2814E+17	1.26	0.577
	44	5.9163E+17	5.3059E+17	1.11	0.991
	45	7.2644E+17	4.8989E+17	1.48	0.965
	46	8.6181E+17	5.1865E+17	1.66	0.852
	48	6.4522E+17	5.3452E+17	1.20	0.987
	49	7.0738E+17	5.3581E+17	1.32	0.892
	52	2.3213E+17	5.8862E+17	2.53	0.059
	54	3.1922E+17	6.1141E+17	1.91	0.229
	55	**2.522E+17**	**5.8639E+17**	**2.32**	**0.02**
	57	3.8624E+17	5.7149E+17	1.47	0.658

Node = node tested for a shift (see Supporting Information S1). Ingroup rate = rate of evolution estimated in the putative shifting clade. Background rate = rate of evolution for the remaining phylogeny outside of the putative shifting clade. Ratio = ratio between the ingroup and the background rate. p-value = significance value of the ratio. Bold p-values indicate cases where the p-value was below the significance threshold of 0.05.

b) Two-shifts models - hindwing

Model	Structure	Rate	Pairwise comparison	Pairwise ratio	Pairwise p-value
1	55	2.52E+17	1_2	2.25	0.29
	33	5.66E+17	1_B	2.37	0.02
	background	5.98E+17	2_B	1.06	0.99
2	55	2.52E+17	1_2	2.79	0.44
	34	7.02E+17	1_B	2.27	0.02
	background	5.71E+17	2_B	1.23	0.97
3	55	2.52E+17	1_2	2.01	0.29
	36	5.07E+17	1_B	2.43	0.02
	background	6.13E+17	2_B	1.21	0.88
4	55	2.52E+17	1_2	2.21	0.15
	38	5.58E+17	1_B	2.35	0.02
	background	5.92E+17	2_B	1.06	0.92
5	55	2.52E+17	1_2	1.70	0.48
	39	4.29E+17	1_B	2.40	0.02
	background	6.06E+17	2_B	1.41	0.67
6	55	2.52E+17	1_2	2.35	0.26
	44	5.91E+17	1_B	2.31	0.03
	background	5.82E+17	2_B	1.02	1.00
7	55	2.52E+17	1_2	2.88	0.24
	45	7.26E+17	1_B	2.09	0.06
	background	5.27E+17	2_B	1.38	0.99
8	55	2.52E+17	1_2	3.42	0.22
	46	8.61E+17	1_B	2.19	0.02
	background	5.51E+17	2_B	1.56	0.86
9	55	2.52E+17	1_2	2.56	0.39
	48	6.45E+17	1_B	2.27	0.01
	background	5.73E+17	2_B	1.13	0.99
10	55	2.52E+17	1_2	2.80	0.23
	49	7.07E+17	1_B	2.27	0.03
	background	5.71E+17	2_B	1.24	0.91
11	55	2.52E+17	1_2	1.09	0.89
	52	2.32E+17	**1_B**	**2.50**	**0.01**
	background	6.30E+17	**2_B**	**2.72**	**0.04**
12	55	2.52E+17	1_2	1.53	0.57
	57	3.86E+17	1_B	2.42	0.02
	background	6.11E+17	2_B	1.58	0.62

Structure = structure of the model, i.e. the node number of the two putative shifts tested and remaining phylogeny outside from the putative shifting clade ("background"). In each case the first node indicated is the node retained in the one-shift model comparisons. Rate = rate of evolution of each part of the model, i.e. two ingroup rates and one background rate. Pairwise comparison = pairs considered in the following pairwise comparison (1-2=ingroup

1 and ingroup 2, 1-B=ingroup 1 and background, 2-B=ingroup 2 and background). Pairwise ratios = ratio between the two rates considered in the pairwise comparison. Pairwise p-value = significance value of the pairwise ratio. Bold p-values indicate the case for which both subclades were significantly different than the background rate.

Supporting Information S4.

A. Results of models with shifts in rates of wing shape evolution for females on the MCC tree.

a) One-shift models

Wing	Node	Ingroup rate	Background rate	Ratio	p-value
Forewing	32	5.49E+19	5.40E+17	101.55	0.001
	33	5.58E+17	1.93E+19	34.67	0.001
	35	8.20E+19	5.43E+17	151.17	0.001
	37	**1.22E+20**	**6.18E+17**	**197.98**	**0.001**
	38	1.60E+20	9.45E+17	169.38	0.001
	40	5.18E+17	4.50E+19	86.97	0.001
	41	5.04E+17	4.13E+19	82.09	0.001
	42	6.09E+17	2.77E+19	45.45	0.001
	43	5.96E+17	2.38E+19	39.97	0.001
	44	6.17E+17	1.93E+19	31.35	0.001
	46	5.83E+17	2.09E+19	35.87	0.001
	47	5.78E+17	1.93E+19	33.48	0.001
	50	6.44E+17	1.93E+19	30.03	0.001
	52	3.11E+17	2.19E+19	70.32	0.001
	55	2.84E+17	1.94E+19	68.29	0.001
Hindwing	32	8.32E+19	8.50E+17	97.89	0.001
	33	7.17E+17	2.93E+19	40.99	0.001
	35	1.25E+20	8.33E+17	149.48	0.001
	37	**1.86E+20**	**9.29E+17**	**199.94**	**0.001**
	38	2.43E+20	1.47E+18	164.93	0.001
	40	8.57E+17	6.82E+19	79.66	0.001
	41	8.56E+17	6.26E+19	73.13	0.001
	42	9.60E+17	4.19E+19	43.71	0.001
	43	1.00E+18	3.61E+19	36.09	0.001
	44	9.08E+17	2.93E+19	32.31	0.001
	46	1.05E+18	3.17E+19	30.04	0.001
	47	1.01E+18	2.93E+19	28.79	0.001
	50	8.54E+17	2.93E+19	34.39	0.001
	52	6.66E+17	3.32E+19	49.75	0.001
	55	8.44E+17	2.93E+19	34.79	0.001

Structure = structure of the model, i.e. the node number of the two putative shifts tested and remaining phylogeny outside from the putative shifting clade ("background"). In each case the first node indicated is the node retained in the one-shift model comparisons. Rate = rate of evolution of each part of the model, i.e. two subclade rates and one background rate. Pairwise comparison = pairs considered in the following pairwise comparison (1_2 = subclade 1 and subclade 2, 1_B = subclade 1 and background, 2_B = subclade 2 and background). Pairwise ratios = ratio between the two rates considered in the pairwise

comparison. Pairwise p-value = significance value of the pairwise ratio. Bold p-values indicate the case for which both subclades were significantly different than the background rate.

b) Two-shifts models - forewing

Model	Structure	Rate	Pairwise comparison	Pairwise ratio	Pairwise p-value
1	37	1.22E+20	1_2	219.22	0.001
	33	5.57E+17	1_B	195.40	0.001
	background	6.25E+17	2_B	1.12	0.95
2	37	1.22E+20	1_2	236.21	0.001
	40	5.17E+17	1_B	139.80	0.001
	background	8.74E+17	2_B	1.68	0.521
3	37	1.22E+20	1_2	242.87	0.001
	41	5.03E+17	1_B	142.15	0.001
	background	8.60E+17	2_B	1.70	0.469
4	37	1.22E+20	1_2	200.93	0.001
	42	6.08E+17	1_B	195.72	0.001
	background	6.24E+17	2_B	1.02	0.99
5	37	1.22E+20	1_2	205.38	0.001
	43	5.95E+17	1_B	194.68	0.001
	background	6.28E+17	2_B	1.05	0.983
6	37	1.22E+20	1_2	198.28	0.001
	44	6.16E+17	1_B	197.94	0.001
	background	6.17E+17	2_B	1.00	1
7	37	1.22E+20	1_2	209.89	0.001
	46	5.82E+17	1_B	195.21	0.001
	background	6.26E+17	2_B	1.07	0.964
8	37	1.22E+20	1_2	211.71	0.001
	47	5.77E+17	1_B	196.25	0.001
	background	6.23E+17	2_B	1.07	0.942
9	37	1.22E+20	1_2	189.97	0.001
	50	6.43E+17	1_B	199.13	0.001
	background	6.14E+17	2_B	1.04	0.96
10	37	1.22E+20	1_2	393.42	0.001
	52	3.10E+17	1_B	171.13	0.001
	background	7.14E+17	2_B	2.29	0.231
11	37	1.22E+20	1_2	361.82	0.001
	53	3.38E+17	1_B	186.47	0.001
	background	6.55E+17	2_B	1.94	0.328
12	37	1.22E+20	1_2	431.07	0.001
	55	2.83E+17	1_B	184.39	0.001
	background	6.63E+17	2_B	2.33	0.333

Structure = structure of the model, i.e. the node number of the two putative shifts tested and remaining phylogeny outside from the putative shifting clade ("background"). In each case the first node indicated is the node retained in the one-shift model comparisons. Rate = rate of evolution of each part of the model, i.e. two subclade rates and one background rate. Pairwise comparison = pairs considered in the following pairwise comparison (1_2 = subclade 1 and subclade 2, 1_B = subclade 1 and background, 2_B = subclade 2 and

background). Pairwise ratios = ratio between the two rates considered in the pairwise comparison. Pairwise p-value = significance value of the pairwise ratio. Bold p-values indicate the case for which both subclades were significantly different than the background rate.

c) Two-shifts models - hindwing

Model	Structure	Rate	Pairwise comparison	Pairwise ratio	Pairwise p-value
1	37	1.86E+20	1_2	259.14	0.001
	33	7.17E+17	1_B	193.90	0.001
	background	9.58E+17	2_B	1.33	0.892
2	37	1.86E+20	1_2	216.81	0.001
	40	8.57E+17	1_B	166.60	0.001
	background	1.11E+18	2_B	1.30	0.747
3	37	1.86E+20	1_2	216.87	0.001
	41	8.56E+17	1_B	171.49	0.001
	background	1.08E+18	2_B	1.26	0.735
4	37	1.86E+20	1_2	193.41	0.001
	42	9.60E+17	1_B	205.38	0.001
	background	9.04E+17	2_B	1.06	0.977
5	37	1.86E+20	1_2	185.70	0.001
	43	1.00E+18	1_B	207.42	0.001
	background	8.95E+17	2_B	1.11	0.964
6	37	1.86E+20	1_2	204.42	0.001
	44	9.08E+17	1_B	199.34	0.001
	background	9.32E+17	2_B	1.02	0.988
7	37	1.86E+20	1_2	176.03	0.001
	46	1.05E+18	1_B	206.96	0.001
	background	8.97E+17	2_B	1.17	0.928
8	37	1.86E+20	1_2	182.23	0.001
	47	1.01E+18	1_B	202.62	0.001
	background	9.17E+17	2_B	1.11	0.946
9	37	1.86E+20	1_2	217.50	0.001
	50	8.54E+17	1_B	197.76	0.001
	background	9.39E+17	2_B	1.09	0.935
10	37	1.86E+20	1_2	278.86	0.001
	52	6.66E+17	1_B	183.53	0.001
	background	1.01E+18	2_B	1.51	0.536
11	37	1.86E+20	1_2	380.70	0.001
	53	4.88E+17	1_B	187.78	0.001
	background	9.89E+17	2_B	2.02	0.336
12	37	1.86E+20	1_2	220.01	0.001
	55	8.44E+17	1_B	197.48	0.001
	background	9.40E+17	2_B	1.11	0.882

Structure = structure of the model, i.e. the node number of the two putative shifts tested and remaining phylogeny outside from the putative shifting clade ("background"). In each case the first node indicated is the node retained in the one-shift model comparisons. Rate = rate of evolution of each part of the model, i.e. two subclade rates and one background rate.

Pairwise comparison = pairs considered in the following pairwise comparison (1_2 = subclade 1 and subclade 2, 1_B = subclade 1 and background, 2_B = subclade 2 and background). Pairwise ratios = ratio between the two rates considered in the pairwise comparison. Pairwise p-value = significance value of the pairwise ratio. Bold p-values indicate the case for which both subclades were significantly different than the background rate.

Supporting Information S5. Results of all time-dependent diversification models fitted on the *Morpho*, the different subscales tested (canopy, monocots, shape shift) and the corresponding backbone trees. *Model* indicates the shape of speciation and extinction rate functions: BCST=constant speciation, BVAR=time-dependent speciation, DCST=constant extinction, DVAR=time-dependent extinction. Par=number of parameters in the model. logL=likelihood of the model. AIC=Akaike Information Criterion. λ =speciation rate at present, α=coefficient of time variation of the speciation rate, μ =extinction rate at present, ß =coefficient of time variation of the extinction rate.

Whole tree

Model	Par	logL	AIC	ΔAIC	λ	α	μ	β
BVAR	2	-96.97	197.95	0.00	0.053	0.047		
BCST	1	-98.40	198.81	0.86	0.081			
BVARDCST	3	-96.97	199.95	2.00	0.053	0.047	0.000	
BCSTDCST	2	-98.40	200.81	2.86	0.081		0.000	
BVARDVAR	4	-96.97	201.95	4.00	0.053	0.047	0.000	0.019
BCSTDVAR	3	-98.40	202.81	4.86	0.081		0.000	0.014

Background without canopy

Model	Par	logL	AIC	ΔAIC	λ	α	μ	β
BCST	1	-67.01	136.03	0.00	0.080			
BVAR	2	-66.10	136.20	0.18	0.053	0.044		
BCSTDCST	2	-67.01	138.03	2.00	0.080		0.000	
BVARDCST	3	-66.04	138.09	2.06	0.060	0.049	0.034	
BVARDVAR	4	-65.75	139.50	3.47	0.144	0.006	1.048	-0.691
BCSTDVAR	3	-67.01	140.03	4.00	0.080		0.000	0.002

Background without monocots

Model	Par	logL	AIC	ΔAIC	λ	α	μ	β
BCST	1	-73.75	149.49	0.00	0.081			
BVAR	2	-73.24	150.48	0.98	0.060	0.031		
BVARDVAR	4	-71.58	151.16	1.66	0.034	0.205	0.039	0.201
BCSTDCST	2	-73.75	151.49	2.00	0.081		0.000	
BVARDCST	3	-72.83	151.65	2.16	0.081	0.051	0.101	
BCSTDVAR	3	-73.75	153.49	4.00	0.081		0.000	-0.039

Background without shape shift

Model	Par	logL	AIC	ΔAIC	λ	α	μ	β
BVAR	2	-76.57	157.13	0.00	0.045	0.054		
BCST	1	-78.18	158.36	1.22	0.078			
BVARDCST	3	-76.52	159.04	1.91	0.051	0.059	0.028	

BCSTDCST	2	-78.18	160.36	3.22	0.078		0.000	
BVARDVAR	4	-76.45	160.89	3.76	0.061	0.047	0.146	-0.287
BCSTDVAR	3	-78.18	162.36	5.22	0.078		0.000	-0.008

Background without monocots and canopy

Model	Par	logL	AIC	ΔAIC	λ	α	μ	β
BVARDVAR	4	-35.68	79.36	0.00	0.063	0.237	0.079	0.228
BCST	1	-39.78	81.57	2.20	0.073			
BCSTDCST	2	-39.39	82.78	3.41	0.119		0.089	
BCSTDVAR	3	-38.70	83.39	4.03	0.180		0.493	-0.154
BVARDCST	3	-39.47	84.94	5.57	0.183	0.045	0.330	
BVAR	2	-42.22	88.43	9.07	0.064	0.020		

Background without monocots and shape shift

Model	Par	logL	AIC	ΔAIC	λ	α	μ	β
BCST	1	-50.91	103.83	0.00	0.072			
BVARDVAR	4	-48.05	104.11	0.28	0.046	0.215	0.061	0.205
BCSTDVAR	3	-49.56	105.13	1.30	0.177		0.668	-0.242
BCSTDCST	2	-50.90	105.80	1.97	0.078		0.013	
BVARDCST	3	-50.72	107.45	3.62	0.124	0.057	0.246	
BVAR	2	-52.90	109.80	5.97	0.050	0.039		

Canopy

Model	Par	logL	AIC	ΔAIC	λ	α	μ	β
BCST	1	-31.39	64.77	0.00	0.083			
BVAR	2	-30.81	65.62	0.84	0.050	0.059		
BCSTDCST	2	-31.39	66.77	2.00	0.083		0.000	
BVARDCST	3	-30.81	67.62	2.84	0.050	0.059	0.000	
BCSTDVAR	3	-31.39	68.77	4.00	0.083		0.000	0.014
BVARDVAR	4	-30.81	69.62	4.84	0.050	0.059	0.000	0.020

Monocots

Model	Par	logL	AIC	ΔAIC	λ	α	μ	β
BVAR	2	-21.78	47.55	0.00	0.014	0.213		
BVARDCST	3	-21.78	49.55	2.00	0.014	0.213	0.000	
BCST	1	-24.66	51.31	3.76	0.080			
BVARDVAR	4	-21.78	51.55	4.00	0.014	0.213	0.000	0.010
BCSTDCST	2	-24.66	53.31	5.76	0.080		0.000	
BCSTDVAR	3	-24.66	55.31	7.76	0.080		0.000	0.010

Shape shift

Model	Par	logL	AIC	ΔAIC	λ	α	μ	β
BCST	1	-20.14	42.28	0.00	0.095			

BVAR	2	-20.09	44.18	1.91	0.081	0.023		
BCSTDCST	2	-20.14	44.28	2.00	0.095		0.000	
BVARDCST	3	-20.09	46.18	3.91	0.081	0.023	0.000	
BCSTDVAR	3	-20.14	46.28	4.00	0.095		0.000	0.029
BVARDVAR	4	-20.09	48.18	5.91	0.081	0.023	0.000	0.037

Supporting Information S6. Adjacency matrix and dispersal matrices time-stratified used for the BioGeoBEARS ancestral state reconstruction. CA=Central America, SN=Sierra Nevada de Santa Maria, W=lowland western Andes, N=Northern Andes, S=Central Andes, NAz=Northern Amazonia, SAZ=Southern Amazonia, AF=Atlantic Forest.

a) Adjacency matrix

	CA	SN	W	N	S	NAz	SAz	AF
CA	1	0	1	1	0	0	0	0
SN	0	1	1	0	0	0	0	0
W	1	1	1	1	1	1	0	0
N	1	1	1	1	1	1	0	0
S	0	1	1	1	0	0	1	1
NAz	0	1	1	0	1	1	1	0
SAz	0	0	0	1	1	1	1	1
AF	0	0	0	1	0	0	1	1

b) Dispersal multipliers matrix

0-5 mya

	CA	SN	W	N	S	NAz	SAz	AF
CA	1	0	1	0	0	0	0	0
SN	0	1	0	0	0	0	0	0
W	1	0	1	0	0	0	0	0
N	0	0	0	1	1	1	1	0
S	0	0	0	1	1	0.1	1	0.5
NAz	0	0	0	1	0.1	1	0.1	0
SAz	0	0	0	1	1	0.1	1	0
AF	0	0	0	0	0.5	0	0	1

5-10 mya

	CA	SN	W	N	S	NAz	SAz	AF
CA	1	0	0	0	0	0	0	0
SN	0	1	0	0	0	0	0	0
W	0	0	1	0.5	0.5	0.25	0	0
N	0	0	0.5	1	0.5	0.5	0.5	0
S	0	0	0.5	0.5	1	0.1	1	0.5
NAz	0	0	0.25	0.5	0.1	1	0.1	0
SAz	0	0	0	0.5	1	0.1	1	0
AF	0	0	0	0	0.5	0	0	1

10-15 mya

	CA	SN	W	N	S	NAz	SAz	AF
CA	1	0	0	0	0	0	0	0
SN	0	1	0.5	0.25	0	0	0	0
W	0	0.5	1	0.5	0.5	0	0	0
N	0	0.25	0.5	1	0	0	0	0
S	0	0	0.5	0	1	1	1	0.5
NAz	0	0	0	0	1	1	1	0
SAz	0	0	0	0	1	1	1	0
AF	0	0	0	0	0.5	0	0	1

15-23 mya

	CA	SN	W	N	S	NAz	SAz	AF
CA	1	0	0.5	0	0	0	0	0
SN	0	1	0.5	0.5	0	0	0	0
W	0.5	0.5	1	1	0.5	0	0	0
N	0	0.5	1	1	0	0	0	0
S	0	0	0.5	0	1	1	1	0.5
NAz	0	0	0	0	1	1	1	0
SAz	0	0	0	0	1	1	1	0
AF	0	0	0	0	0.5	0	0	1

23-30 mya

	CA	SN	W	N	S	NAz	SAz	AF
CA	1	0	0	0	0	0	0	0
SN	0	1	0.5	0.5	0	0	0	0
W	0	0.5	1	1	0.5	0	0	0
N	0	0.5	1	1	0.5	0	0.5	0
S	0	0	0.5	0.5	1	1	1	0.5
NAz	0	0	0	0	1	1	1	0.5
SAz	0	0	0	0.5	1	1	1	0.5
AF	0	0	0	0	0.5	0.5	0.5	1

1084
1085